

**OVER-EXPRESSION OF APOPTOSIS INHIBITOR 5 (API5) RESULTS IN
TRANSFORMATION OF BREAST EPITHELIAL CELLS**

Bodakuntla Satish

Reg. No. 20091091, IISER Pune



A thesis submitted in partial fulfillment of the requirements
for the BS-MS dual degree programme in IISER Pune

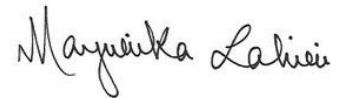
Research Advisor:

Dr. Mayurika Lahiri, Assistant Professor

Biology Division, IISER Pune

Certificate

This is to certify that this dissertation entitled 'Over-expression of Apoptosis inhibitor 5 (Api5) results in transformation of breast epithelial cells' towards the partial fulfillment of the BS-MS dual degree programme at the Indian Institute of Science Education and Research (IISER), Pune represents original research carried out by Bodakuntla Satish at IISER Pune under the supervision of Dr. Mayurika Lahiri, Assistant Professor, Biology Division, IISER Pune during the academic year 2014-2015.



Dr. Mayurika Lahiri

Assistant Professor

Biology Division, IISER Pune

Declaration

I hereby declare that the matter embodied in the thesis entitled 'Over-expression of Apoptosis inhibitor 5 (Api5) results in transformation of breast epithelial cells' are the results of the investigations carried out by me at the Biology Division, IISER Pune under the supervision of Dr. Mayurika Lahiri, Assistant Professor, Biology Division, IISER Pune and the same has not been submitted elsewhere for any other degree.



Bodakuntla Satish

20091091

BS-MS Dual Degree Student

IISER Pune

Abstract

Api5 has been reported to be a metastatic oncogene in several cancers. However, till date, its role in breast cancer is poorly understood. Initially identified as an inhibitor of apoptosis, Api5 has also been found to enhance cellular proliferation. The primary aim of this study was to establish the role of Api5 in breast epithelial cell transformation. Three-dimensional (3D) culture of MCF10A cells, a model system biologically more relevant than traditional models, was used to answer this question. Over-expression of Api5 resulted in larger acinar structures with increased cellular proliferation and partial clearing of luminal space probably due to delayed apoptosis. These phenotypes were indicative of transformation and resembled early lesions in breast cancer. Apart from this, loss of apico-basal polarity and integrity of cell-cell junctions coupled with up-regulation of vimentin were some the key features that were observed, which indicated EMT-like phenotype. This observation was further supported by the formation of protrusion-like or 'bulb-like' structures. Inability of the cells to form acinar structures upon alteration of matrix stiffness further strengthened our claim that up-regulation of Api5 is sufficient to induce transformation in non-malignant breast epithelial cells. Collectively, this study demonstrated the possible role of Api5 in breast epithelial cell transformation, which may serve as a novel target for treatment of breast cancer.

Table of Contents

Certificate	ii
Declaration	iii
Abstract	iv
Table of Contents	v
List of Figures	vii
Acknowledgements	viii
Introduction	1
Breast cancer	1
Api5 and its role in Cancer.....	2
Breast epithelial 3D culture as a model system	4
Aims and objectives of this study.....	8
Materials and Methods:	9
Chemicals and antibodies.....	9
Cell lines and culture conditions	9
3D on-top culture	10
3D culture immunofluorescence	10
Immunoblot analysis	11
Lentivirus production and transduction using calcium phosphate method	12
Lentivirus production and transduction using Effectene transfection reagent ..	13
Statistical Analysis	14
Results:	15
Differential expression of Api5 levels in MCF10A series.....	15
Generation of a stable cell line of MCF10A over-expressing Api5.....	16
Api5 over-expression resulted in increase in acinar size with enhanced cellular proliferation.....	20
Api5 over-expression caused disruption of Apico-Basal polarity	26

Api5 over-expression disrupted cell-cell junctions.	30
Api5 over-expression induced up-regulation of Vimentin, an Epithelial to Mesenchymal transition (EMT) marker.	33
Api5-MCF10A cells seeded on Collagen-Matrigel® failed to form acini.....	35
Discussion:	37
Future perspectives	39
References:	41

List of Figures

Figure 1: Global statistics of cancer incidence and mortality rates in females.	1
Figure 2: Anatomy of a mammary epithelium..	5
Figure 3: Various possible phenotypes of 3D cultures of non-malignant breast epithelial cells and malignant breast epithelial cells	7
Figure 4: Api5 levels across cell lines belonging to MCF10A series.	15
Figure 5: Representative image of transduced HEK 293T cells.....	17
Figure 6: Sorting of Api5-MCF10A cells fluorescing mCherry.....	17
Figure 7: Api5 levels in Api5-MCF10A	19
Figure 8: Morphological differences between MCF10A and Api5-MCF10A cells	19
Figure 9: Over-expression of Api5 leads to increase in size of the acini	21
Figure 10: Api5 over-expression leads to increase in number of cells per acini..	22
Figure 11: Api5 over-expression results in enhanced proliferation.....	23
Figure 12: Api5-MCF10A cells form acini with partially cleared lumen.....	24
Figure 13: Api5 over-expression does not affect nuclear size.....	25
Figure 14: Api5 over-expression disrupts apical polarity.....	27
Figure 15: Api5 over-expression results in loss of α 6-Integrin.....	28
Figure 16: Api5 over-expression results in loss of Laminin V.....	29
Figure 17: Api5 over-expression leads to loss of E Cadherin, cell-cell junction protein.....	31
Figure 18: Api5 over-expression leads to loss of α -Catenin, cell-cell junction protein.....	32
Figure 19: Api5 over-expression results in up-regulation of Vimentin, an EMT marker.....	34
Figure 20: Api5 over-expression results in formation of migratory or invasive 3D structures.	36
Figure 21: Suggested pathways that may be involved in observed phenotypes upon Api5 over-expression.	40

Acknowledgements

Working in this lab for the past four years, I have been exposed significantly to the thrills and excitements of scientific research. It wouldn't be possible to finish this exciting journey without the support and encouragement of my colleagues.

Firstly I would like to express my sincere gratitude to Dr. Mayurika Lahiri for giving me the golden opportunity to be a part of her lab, for her constant support and tremendous encouragement, for her boundless patience in listening and answering my trivial questions, for being friendly and for her inspiring guidance throughout the period of my work. I consider myself one of the very fortunate people to be associated with her. This opportunity means a lot to me in life. If I had to write whatever I want to write about this amazing lady, it will probably take a year to finish.

I would like to thank Dr. Manas Santra, NCCS for his help with preparation of stable cell line. I would like to thank my thesis advisory committee member, Dr. Sorab Dalal, for his valuable suggestions.

Next, I would like to whole heartedly thank my friend Libi Anandi, without whom I wouldn't have been able to complete my thesis. I would like thank her for establishing 3D cultures and standardizing its various staining protocols, which made my life relatively easier. I would like to thank her for listening to some of my difficult times with utmost patience, for her constructive criticism and useful discussions about the project, for her support and encouragement all throughout my period of project. I will never forget this.

I would also like to thank Surojit Sural, for his encouragement, for his all the help with 'Alkylation damage' projects and for sharing his valuable knowledge about the field with me.

I would also like to sincerely thank Vaishali, and Ashiq, for helping me out with experiments and for their useful discussions. I would also like to extend my sincere thanks to all the present as well as ex-members of the Lahiri Lab.

I would also like to thank Kishore Vaigyanik Protsahan Yojana (KVPY) and IISER, Pune for providing financial support.

I would like to thank my family members for their support and encouragement throughout my academic career in IISER, Pune. I am also thankful to Kaniganti and Priyatam, for their entertaining and intriguing discussions at '*Bhurji Bandi*' after the tiring days in the lab.

I would like to thank Vijay and IISER Pune microscopy facility. I am grateful to the Biology Department of IISER, Pune for providing me with all the facilities and opportunities required for my thesis. This is definitely one of the best places in the country for research.

Introduction

Breast cancer

According to global cancer statistics by World Health Organization (WHO) in 2012, breast cancer is the second most common cancer and is the leading cause of cancer death in women (Figure 1).

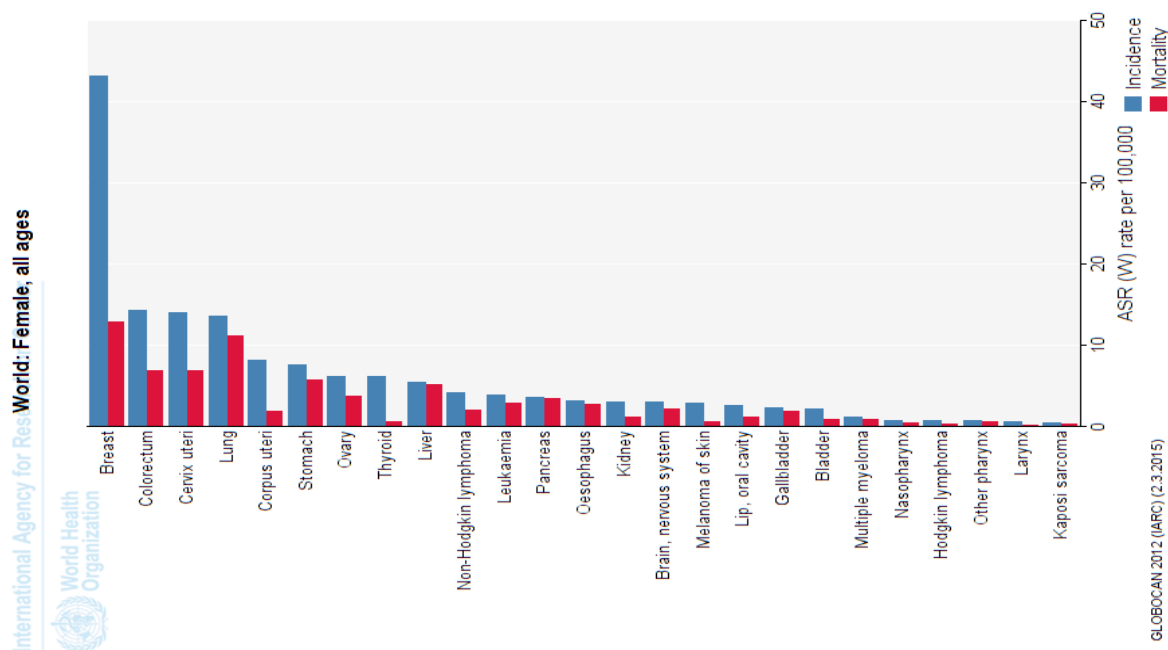


Figure 1: Global statistics of cancer incidence and mortality rates in females.

Reproduced from GLOBOCAN 2012 (IARC); *Section of Cancer Surveillance*.

Breast cancer is known to be caused by the effect of both genetic as well as non genetic factors like tobacco use, diet and environmental exposure to radiation. Though, there has been a significant advancement in breast cancer research, still, the major pathways activated in cancer progression and metastasis, are not yet completely understood (Tinoco et al., 2013). While the levels of multiple gene products have been altered in breast cancers as compared to normal tissue, the significance of these alterations is not clear. Deregulation of DNA repair genes such as BRCA1 (Meijers-Heijboer et al., 2002; Thompson and Easton, 2002; Welch and King, 2001) and BRCA2 (Meijers-Heijboer et al., 2002; Welch and King, 2001), cell-cell junction protein such as E-Cadherin (Guilford et al., 1998),

cell polarity regulators such as STK11/LKB1 (Hemminki et al., 1998; Jenne et al., 1998) and apoptosis regulators such as p53 (Malkin et al., 1990) results in increased risk of breast cancer development. Also, other genes most commonly associated with breast cancer are BRIP1 (Seal et al., 2006; Turnbull and Rahman, 2008), PALB2 (Rahman et al., 2007), ATM (Renwick et al., 2006; Turnbull and Rahman, 2008), MRE11A (Damiola et al., 2014), CHEK2 (Meijers-Heijboer et al., 2002; Turnbull and Rahman, 2008), BARD1 (Ratajska et al., 2012), RAD50 (Damiola et al., 2014), NBN (Damiola et al., 2014), and PTEN (Nelen et al., 1997). In addition to these genes, current research has revealed few breast cancer associated novel genes including, DBC1, BCL11A, SALL1, EPSTI1, CIDE-A, CFBF, MYH9, FBLN2, RUNX1, API5, MLL3, SF3B1 and EMILIN2 (Ellis et al., 2012; Hill et al., 2010; Jansen et al., 2005; Khaled et al., 2015; Ramdas et al., 2011). Although some of these genes have been considerably studied in other types of cancers their role in breast cancer has not been explored. One such gene is Api5, whose role in breast cancer is poorly studied while in other types of cancers, is well-studied.

Api5 and its role in Cancer

Apoptosis inhibitor 5 (Api5), also known as anti apoptosis clone 11 (AAC11) and fibroblast growth factor-2-interacting factor (FIF) is a nuclear protein primarily known for its anti apoptotic function (Van den Berghe et al., 2000). Api5 gene is located at chromosome 11p11.2 and is found to be conserved across different species (Han et al., 2012). It was first identified as a novel cDNA, whose ectopic expression enhanced cell survival in growth factor deprived cervical cancer cells (Tewari et al., 1997) and evaded apoptosis induced by DNA damaging agents (Rigou et al., 2009). Api5 has been found to be up-regulated in multiple tumor types including colon, liver, pancreas, stomach, kidneys, esophagus (Koci et al., 2012), lung (Sasaki et al., 2001; Wang et al., 2010), B-cell chronic lymphoid leukemia (Krejci et al., 2007) and cervical cancer (Kim et al., 2000). Kim and colleagues, using adhesion and invasion assays, identified Api5 over-expression to induce invasion of cervical cancer cells, possibly through its role in cell interactions with extracellular matrix (Kim et al., 2000). They also showed that Api5 levels were inversely co-related to loss of tissue inhibitor of

metalloproteinase1 (TIMP-1) and TIMP-2. Further studies by Song *et al.* have elucidated the mechanisms through which Api5 induces invasion in cervical cancer cells. They showed that Api5 over-expression activates ERK signaling pathway, which in turn enhances MMP9 secretion, eventually leading to invasion (Song *et al.*, 2014).

A protein belonging to the same family as that of Api5, called Api4, also known as Survivin is an anti-apoptotic protein shown to be up-regulated in various cancers including bladder cancer (Swana *et al.*, 1999), cervical cancer (Lee *et al.*, 2005), colon cancer (Kim *et al.*, 2003), and others. Although both Api4 and Api5 belong to same family of proteins, the role of Api5 in breast cancer is not well studied while role of Survivin is extensively explored. However, there are only two studies that indirectly support the role of Api5 in breast cancer. First, up-regulation of Api5 was observed in tamoxifen resistant breast cancer cells (Jansen *et al.*, 2005). Later Ramdas and colleagues have shown that Api5 was down-regulated in tocotrienol-treated human breast cancer MCF7 cells which mediated tocotrienol induced cell death (Ramdas *et al.*, 2011).

Further, it was also shown that down regulation of Api5 in various cancer cell lines including, colon cancer (HCT116), osteosarcoma (U20S), lung adenocarcinoma (A549) and cervical cancer (HeLa) cells resulted in increased sensitivity to apoptosis (Morris *et al.*, 2006; Rigou *et al.*, 2009; Wang *et al.*, 2010). Noh *et al* have showed that tumor cells use Api5 to resist apoptosis induced by tumor antigen-specific T cells (Noh *et al.*, 2014). They also showed that Api5 mediated resistance to apoptosis is via up-regulation of FGF2 secretion, leading to activation of FGFR1 receptor signaling, resulting in activated ERK dependant degradation of a pro-apoptotic molecule, BIM (Noh *et al.*, 2014). This study not only demonstrated the role of Api5 over-expression in cancer cells but also has revealed one of the mechanisms through which Api5 inhibits apoptosis. In addition to this mechanism, Morris *et al* have showed that Api5 is a negative regulator of E2-promoter binding factor 1 (E2F1) transcription factor induced apoptosis (Morris *et al.*, 2006) while Rigou and his colleagues showed that Api5, when oligomerises, physically interacts with Acinus, a protein involved in the

process of DNA fragmentation. Api5-Acinus complex thus formed prevents cleavage of Acinus by caspase and protects DNA from fragmentation (Rigou et al., 2009). In addition to its role in apoptosis and invasion, Api5 was also observed to regulate E2F1 transcriptional activation of G/S cell cycle transition genes by enhancing its binding affinity to its target promoter (Garcia-Jove Navarro et al., 2013).

Thus, the anti-apoptotic role and probable oncogenic role of Api5 along with its implicated role in cell cycle, makes it an interesting candidate for studying its role in breast tumorigenesis. To achieve this, we plan to use 3D cultures that have emerged as a powerful tool to study breast tumorigenesis.

Breast epithelial 3D culture as a model system

Glandular epithelium, such as mammary gland comprises of many individual glandular units called acini, smallest unit of mammary gland *in vivo*. These acinar structures have various distinct features including a hollow lumen surrounded by polarized epithelial cells, maintenance of special cell-cell contacts such as tight junctions, adherent junctions and desmosomes as well as cell-matrix contacts such as hemidesmosomes (Vidi et al., 2013).

The development and maintenance of such intact and well organized structures is critical for the function of epithelial cells. Any alterations in the tissue architecture of this polarized epithelium would lead to occurrence of carcinomas (Bissell and Radisky, 2001).

Three-dimensional (3D) cultures of breast epithelial cells recapitulate the microenvironment of breast tissue present *in vivo*. In this model system, cells are grown on extracellular matrix so as to form functional structures called acini resembling the acini of the mammary gland. (Figure 2a, Figure 2b and Figure 2c).

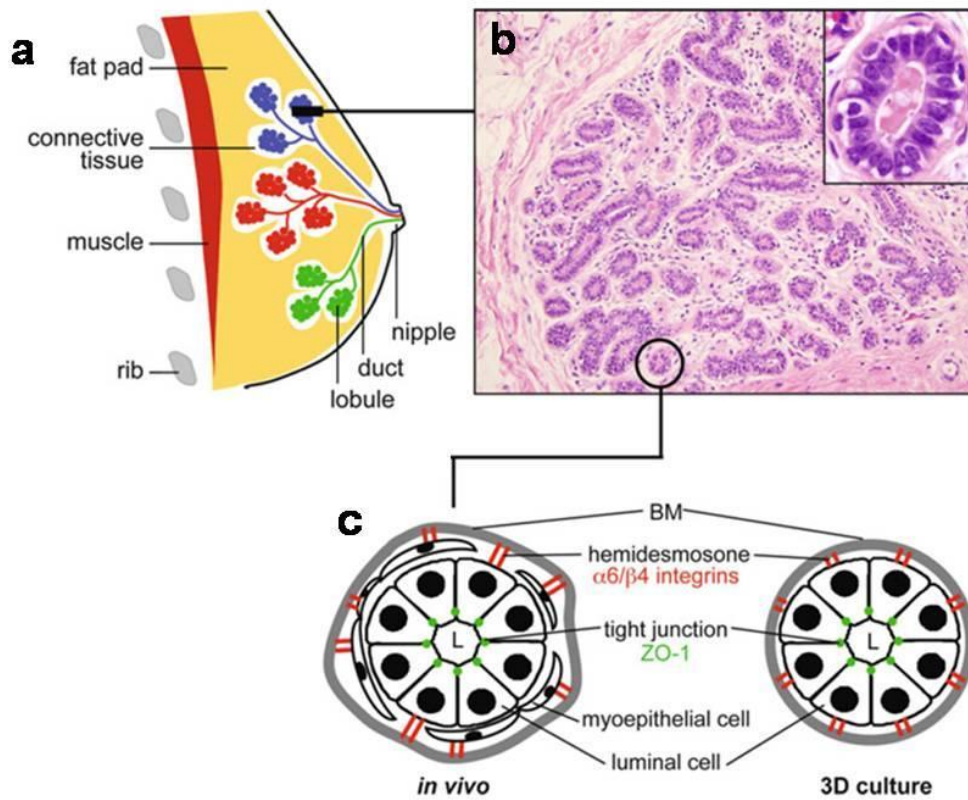


Figure 2: Anatomy of a mammary epithelium. (a) Schematic description of mammary gland with distinct ductal systems connecting to the nipple is shown. (b) Breast lobule's cross section stained with hematoxylin and eosin (H and E) is shown. (c) Schematic and structural comparison of the cross sections of acini *in vivo* and in 3D culture. Image adapted from Vidi *et al.*, 2013.

In the past few decades, increasing number of cancer biologists have been using 3D cultures to elucidate phenotypic and functional effects of oncogenes and tumor suppressor genes. Studies suggest that a mutation in a single gene or small subset of genes is sufficient to disrupt the polarized MCF10A acinar structures illustrating the importance of the model system (Mills et al., 2004; Reginato et al., 2005).

Malignant cells when grown on extra cellular matrix may give rise to different phenotypes such as formation of acini with partially cleared lumen or multiple lumen(Zhang et al., 2011), protrusion like phenotype (Klos et al., 2014) and may also lead to formation of multi-acinar structures as illustrated in figure 3. Such phenotypes have been observed while studying various genes. For instance, activation of ErbB2 oncogene during epithelial cell morphogenesis resulted in formation of multi-acinar structures, as shown schematically in figure 3. It has been proposed that escape from apoptosis and hyper proliferation of cells may be one of the causes for formation of such phenotype (Muthuswamy et al., 2001).

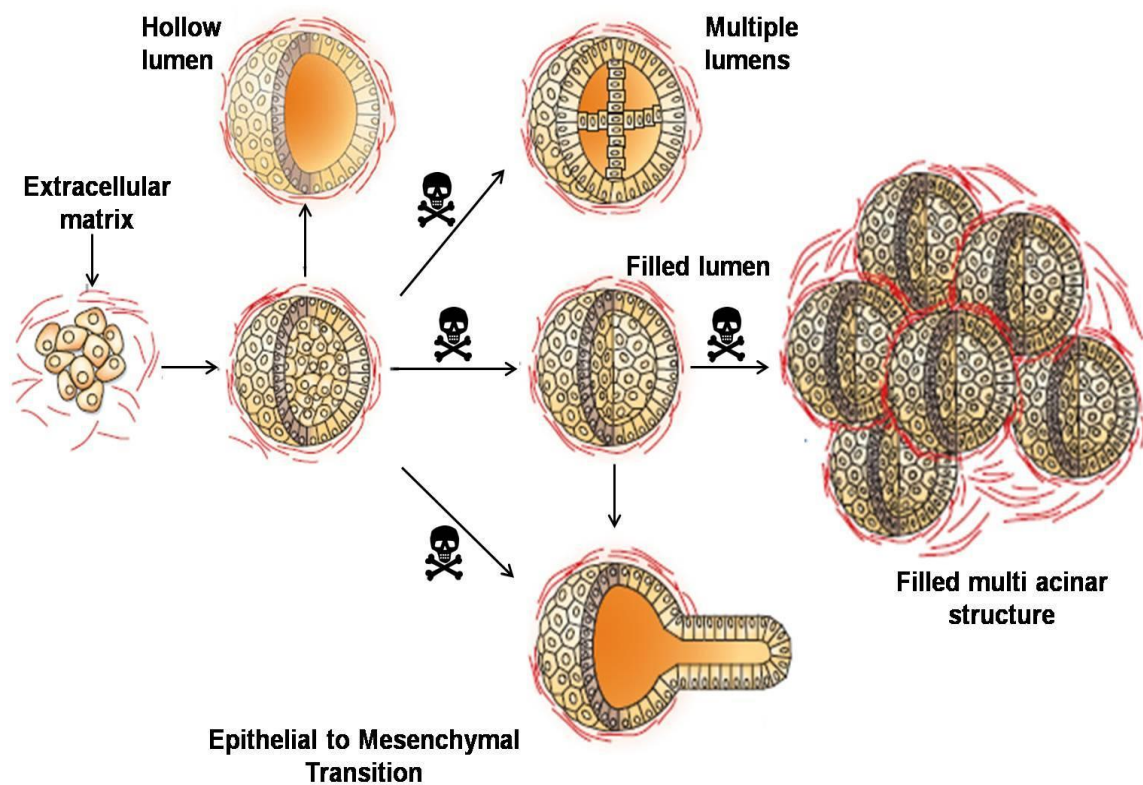


Figure 3: Various possible phenotypes of 3D cultures of non-malignant breast epithelial cells and malignant breast epithelial cells. The figure here demonstrates various morphological changes that may occur upon transformation of non-malignant breast epithelial cells. Transformed cells when grown on Matrigel[®] can give rise to various structures like acini with filled lumen, with multiple lumens, with protrusion like phenotype (an indication of epithelial to mesenchymal transition (EMT)) and filled multi acinar structure. Image adapted from Debnath *et al.*, 2005.

Aims and objectives of this study

The overall aim of this project is to understand the role of Api5 in breast tumorigenesis.

Specific objectives of the study

- Generation of stable cell line of MCF10A over-expressing Api5 (Api5-MCF10A).
- Investigate phenotypic changes induced upon Api5 over-expression
 - Morphometric analysis
 - Effect on apico-basal polarity
 - Effect on cell-cell junctions
 - Induction of invasion

Materials and Methods:

Chemicals and antibodies

N, N-bis [2-hydroxyethyl]-2-aminoethanesulfonic acid (BES), Sodium phosphate dibasic, Calcium chloride, HEPES sodium salt, 1,4-Dithioerythritol (DTE), bromophenol blue, acrylamide, N,N'-methylenebisacrylamide, Trizma[®] base, sodium dodecyl sulfate (SDS), N,N,N',N'-tetramethylethylenediamine (TEMED), sodium azide, Tween 20 and ethylenediaminetetraacetic acid (EDTA) were all purchased from Sigma-Aldrich. Sodium chloride, glycerol, Glycine, sodium hydroxide, potassium chloride, hydrochloric acid and methanol were obtained from Fisher Scientific. Triton-X-100 was bought from USB Corporation. 16% Paraformaldehyde (PFA) solution was bought from VWR International. Goat serum and Precision Plus Protein Dual Color Standards were purchased from Abcam. Polyclonal Api5 antibody was bought from Abnova. Monoclonal antibody for GAPDH was bought from Sigma. Monoclonal antibody for α 6-integrin and GM130 were purchased from Millipore and BD Biosciences, respectively. Monoclonal antibodies for Ki67, Vimentin, E-Cadherin and β -Catenin were purchased from Abcam. AffiniPureF(ab')₂ fragment goat anti-mouse IgG and peroxidase-conjugated AffiniPure goat anti-mouse and anti-rabbit IgG (H+L) were obtained from Jackson Immuno Research. Hoechst 33342 trihydrochloridetrihydrate, Alexa Fluor 488 Goat anti-mouse IgG (H+L), Alexa Fluor 633 Goat anti Rabbit IgG (H+L), Alexa Fluor 488 Goat anti Rat IgG (H+L) and Alexa Flour 633 Phalloidin were bought from Invitrogen.

Cell lines and culture conditions

HEK 293T cell line was a kind gift from Dr. Jomon Joseph (National Centre for Cell Science). HEK 293T cells were grown as monolayer cultures in High Glucose Dulbecco's Modified Eagle Medium (DMEM; Lonza) containing L-glutamine supplemented with 10% heat inactivated fetal bovine serum (FBS; Invitrogen), and 50 units/ml penicillin-streptomycin (Invitrogen). MCF10A cell line was a generous gift from Prof. Raymond C. Stevens (The Scripps Research Institute, California). MCF10A cells were grown as monolayer cultures in Growth Medium which is a composition of High Glucose DMEM without sodium pyruvate

(Invitrogen) supplemented with 5% heat inactivated horse serum (Invitrogen), 0.5 µg/ml hydrocortisone (Sigma-Aldrich), 10 µg/ml insulin (Sigma-Aldrich), 100 ng/ml cholera toxin (Sigma-Aldrich), 20 ng/ml EGF (Sigma-Aldrich) and 100 units/ml penicillin-streptomycin (Lonza). During sub-culturing, MCF10A cells were re-suspended in Resuspension Medium (High Glucose DMEM without sodium pyruvate containing 20% horse serum and 100 units/ml penicillin-streptomycin). All cell lines were maintained in 100 mm tissue-culture treated dishes (Corning) in humidified 5% CO₂ incubator (Thermo Scientific or Eppendorf) at 37°C. For long term storage in liquid nitrogen, HEK 293T cells were stored in DMEM containing 10% DMSO and 20% FBS while MCF10A cells in DMEM (without Sodium pyruvate) containing 5% DMSO and 10% FBS.

3D on-top culture

Wells in 8-well chamber cover glass slides coated with 50 µl growth factor reduced basement membrane matrix (or Matrigel[®]; BD Biosciences) was allowed to polymerize at 37°C for 15-20 minutes. MCF10A cells and Api5 over-expressed MCF10A cells suspended in Assay medium (DMEM without sodium pyruvate containing 2% horse serum, 0.5 µg/ml hydrocortisone, 100 ng/ml cholera toxin, 10 µg/ml insulin and 100 units/ml penicillin-streptomycin) were seeded at equal density of 0.6×10^4 cells per well. Cultures were maintained for 16 days at 37°C and replenished every 4 days with assay medium freshly supplemented with 2% Matrigel[®] and 5 ng/ml EGF.

3D culture immunofluorescence

Medium from 3D on-top cultures was carefully removed using pipettes. Wells were rinsed twice with PBS. When staining for apically and basolaterally localized proteins, acini were incubated with 200 µl of ice-cold PBS-EDTA (PBS containing 5 mM EDTA, 1 mM sodium orthovanadate, 1.5 mM sodium fluoride and 1X protease inhibitor cocktail) for 15 minutes to dissolve Matrigel[®]. This step aids in better penetration of antibodies. After 15 minutes of incubation, majority of supernatant from the wells was carefully removed and were fixed using freshly prepared 4% PFA (pH 7.4) in PBS containing 0.06% glutaraldehyde for 20

minutes at RT. However, PBS-EDTA treatment step was avoided while staining for basement membrane proteins and the acini were directly fixed after the initial PBS washes. Further, wells were washed thrice with 1X PBS for 10 minutes at RT. For permeabilization, wells were incubated with ice-cold PBS containing 0.5% Triton-X-100 for 10 minutes at 4°C and were washed thrice with 1X PBS-Glycine (PBS containing 100 mM glycine) for 10 minutes each. Cultures were then first blocked with primary blocking solution (10% [v/v] goat serum in 1X immunofluorescence (IF) buffer (1X PBS containing 0.05% [w/v] sodium azide, 0.1% [w/v] BSA, 0.2% [v/v] Triton-X-100 and 0.05% Tween 20) for 60 minutes at RT and later with secondary blocking solution (primary blocking solution containing 1% F(ab')₂ fragment goat anti-mouse IgG) for 60 minutes at RT. Cultures were then stained with primary antibody prepared in primary blocking solution, GM130 (1:100) or α 6-integrin (1:100) or β -catenin (1:100) or Ki67 (1:100) or Vimentin (1:100) or E-Cadherin (1:100) or Laminin V (1:100); for 16 hours at 4°C. Wells were washed three times with IF buffer for 20 minutes each at RT. Slides were incubated with secondary antibody prepared in primary blocking solution, Alexa Fluor[®] 488 conjugated Goat anti-rat (1:200), Alexa Fluor[®] 488 conjugated goat anti-mouse IgG (1:200), Alexa Fluor[®] 633 conjugated goat anti-mouse IgG (1:200), Alexa Fluor[®] 488 conjugated goat anti-rabbit IgG (1:200) and 633 conjugated goat anti-rabbit IgG (1:200); for 45-60 minutes at RT. Cultures were washed once with 1X IF buffer for 20 minutes and twice with 1X PBS for 10 minutes at RT. Cultures were counterstained with 1X PBS containing 0.5 μ g/ml Hoechst 33342 for not more than 5 minutes and were washed with 1X PBS for 10 minutes at RT. Cultures were mounted with Slow fade antifade reagent (Molecular probes) and were allowed to set overnight at RT. 3D spheroids were visualized and captured using 63X oil-immersion objective under a Zeiss LSM 710 laser scanning confocal microscope.

Immunoblot analysis

Cell lysates were collected in 2X sample buffer and stored at -40°C. Referring the manufacturer's protocol, a SE 260 mini-vertical gel electrophoresis unit (GE Healthcare) was used to setup Sodium dodecyl sulphate polyacrylamide gel

electrophoresis (SDS-PAGE). 10% resolving gel comprising (9.86% acrylamide, 0.14% bisacrylamide, 475 mM Tris, pH 8.8, 0.1% SDS, 0.1% APS and 0.04-0.08% (v/v) TEMED) and 5% stacking gel comprising of 4.93% acrylamide, 0.07% bisacrylamide, 125 mM Tris, pH 6.8, 0.1% SDS, 0.1% APS and 0.1% [v/v] TEMED was used. Lysates were heated at 95°C and spun at 12,100 X g for 1 minute at room temperature (RT). Samples were loaded onto the gels and were resolved at 120 V. Immobilon-P polyvinylidene difluoride (PVDF) membranes (Millipore) were used to set up the blot transfer in TE22 mighty small transphor unit (GE Healthcare) at 250 mA for 3 hours. 5% (w/v) skimmed milk (SACO Foods, US) prepared in 1X tris buffered saline (TBS; 25 mM Tris (pH 7.6), 150 mM NaCl and 2 mM KCl) containing 0.1% Tween 20 (1X TBS-T) was used to block the PVDF membrane for 1 hour at RT with gentle rocking. Blots were incubated in primary antibody solution for 3 hours at RT (or for 16 hours at 4°C) with gentle rocking. Api5 (1:2500) and GAPDH (1:20000) antibodies were prepared in blocking solution. Blots were washed four times with 1X TBS-T for 10 minutes each and were incubated with peroxidase-conjugated secondary antibody solution (1:10000) prepared in blocking solution for 1 hour at RT with gentle rocking. Blots were again washed four times with 1X TBS-T, developed using Immobilon Western Detection Reagent kit (Millipore) and visualized using Fuji LAS 4000 (GE Healthcare).

Lentivirus production and transduction using calcium phosphate method

For virus production, 2×10^6 HEK 293T cells were seeded on Matrigel[®] coated 100 mm dishes. Matrigel[®] coating was done by incubating tissue-culture treated dishes (Corning) with Matrigel[®] diluted with PBS (1:200) for 16 hours at RT. The dishes were washed thrice with PBS. HEK 293T cells were transfected 16 hours after seeding. 17 μ g of CSII EF MCS Api5 mCherry, 10 μ g of pCMV-VSV-G-RSV-Rev and 10 μ g of pCAG-HIVgp were mixed in 450 μ l of ultrapure DNase RNase free water (Invitrogen). 50 μ l of 2.5 M CaCl₂ was added drop-wise to the plasmid mixture followed by addition of 500 μ l of 2X BBS and mixed gently. Calcium phosphate-DNA mixture was incubated for 20 minutes at RT and was then added to HEK 293T cells and mixed by gentle swirling of the plate. After 16 hours,

media was removed and fresh DMEM supplemented with 10% FBS was added. 48 hours post transfection, virus containing medium was collected, filtered through a 0.45 µm filter and was transferred to a conical ultracentrifuge tube (Beckman 358126) which suits Beckman SW28 rotor including conical inserts (Beckman 358156). The tubes were centrifuged at 50,000g for 2 hours at 4°C and the pellet formed was re-suspended in 600 µl of growth medium containing High Glucose DMEM without sodium pyruvate (Invitrogen) comprising 5% heat inactivated horse serum (Invitrogen), 0.5 µg/ml hydrocortisone, 10 µg/ml insulin, 100 ng/ml cholera toxin, 20 ng/ml EGF and 100 units/ml penicillin-streptomycin. Virus suspension was stored at -80°C. To determine the titre of viral solution, HEK 293T cells were seeded in 24-well plate at a density of $\sim 5 \times 10^4$ cells per well. After 24 hours, different volumes of viral supernatant including 1 µl, 5 µl, 10 µl, 20 µl was added to the different wells. Next day, 1 ml of media was added to each transduced well. On day 5, percentage of cells showing fluorescence in ten randomly selected fields was calculated. If 1 µl of virus solution transduces 10% of the 'y' cells, titre of the viral solution is $(0.1 \times y) \times 10^3$ /ml. Multiplicity of infection (MOI) was calculated using the below formula

$$\text{MOI} = \frac{\text{Volume of viral supernatant (ml)} \times \text{Titre (TU/ml)}}{\text{Target number of cells to be infected}}$$

MOI of 6 is usually preferred for lentivirus transduction and was used to determine the amount of virus solution required. For transduction, MCF10A cells seeded in 100 mm dishes at 70% confluency were used. Next day, medium in the dish was replaced with 6 ml of fresh growth medium. Required amount of viral solution (MOI of 6) was added into the dishes and incubated for 48 hours. After 48 hours, cells were re-fed with fresh medium.

Lentivirus production and transduction using Effectene transfection reagent

100 mm tissue-culture treated dishes coated with Matrigel[®] for 16 hours at RT were washed thrice with PBS before seeding cells. 2×10^6 HEK 293T cells were seeded on Matrigel[®] coated dishes using High Glucose DMEM without sodium

pyruvate (Invitrogen) comprising 5% heat inactivated horse serum (Invitrogen), 0.5 µg/ml hydrocortisone, 10 µg/ml insulin, 100 ng/ml cholera toxin, 20 ng/ml EGF and 100 units/ml penicillin-streptomycin. 4.25 µg of CSII EF MCS Api5 mCherry, 2.5 µg of pCMV-VSV-G-RSV-Rev and 2.5 µg of pCAG-HIVgp was co-transfected in HEK 293T cells using Effectene transfection reagent manufacturer's protocol. Briefly, lentiviral vector with gene of interest along with its packaging plasmids were mixed in 320 µl of buffer EC and 32 µl of Enhancer and the mixture was left undisturbed at RT for 5 minutes. Later, 120 µl of Effectene transfection reagent was added to DNA-Enhancer mixture and was incubated for 30 minutes at RT. Mean while, medium in the plate was removed, washed twice with PBS and fresh 7 ml of growth medium was added. After 30 minutes, 1 ml of growth medium was added to the DNA-Effectene mixture and the transfection mix was added drop-wise by gently swirling of the dish. 48 hours post transfection, virus containing medium was collected, filtered through a 0.45 µm filter, added directly to recipient MCF10A cells. After 48 hours, cells were re-fed with fresh growth medium.

Statistical Analysis

Morphometric analysis for different parameters was calculated from at least three independent experiments. Results for volume and surface area of acini, volume and surface area of nucleus and number of cells per acini were analyzed using Mann Whitney U test, non-parametric test. Data was analyzed and graphs were plotted using GraphPad Prism software (GraphPad Software, La Jolla, CA, USA), and $p < 0.05$ has been used to analyze the statistical significance of parameters between MCF10A and Api5-MCF10A cells.

Results:

Differential expression of Api5 levels in MCF10A series.

MCF10 series constitutes a unique model to study breast cancer progression. It is a series of cell lines derived from MCF10A cells. The series comprises of three cell lines namely non-tumorigenic MCF10A; pre-malignant MCF 10AT1 (Dawson *et al.*, 1996) derived by transfection of MCF10 A with HRAS; and finally MCF10-CA1a derived from MCF10AT1 after multiple passages in nude mice (Santner *et al.*, 2001). Each of the cell lines in the series mimics a clinical stage in breast cancer. MCF10-CA1a is the most aggressive cell line which rapidly develops large tumors and also metastasizes to lungs. The MCF10 cell lines provide the scope to study the genetic alterations (Kadota *et al.*, 2010; Ma *et al.*, 2003) and molecular changes (Rhee *et al.*, 2008) that occur during cancer progression. Hence, we investigated endogenous levels of Api5 protein across the 10A series including MCF10A, MCF10AT1, and MCF10-CA1a. MCF10AT1 cells did not show a significant difference in Api5 protein levels as compared to MCF10A cells. However, the levels in MCF10-CA1a cells were 4 times higher than that of MCF10A cells (Figure 4), thus indicating Api5 levels are perturbed in breast cancer.

Therefore, to study role of Api5 in breast tumorigenesis we over-expressed Api5 in MCF10A cells to partially phenocopy the invasive MCF10-CA1a cell line.

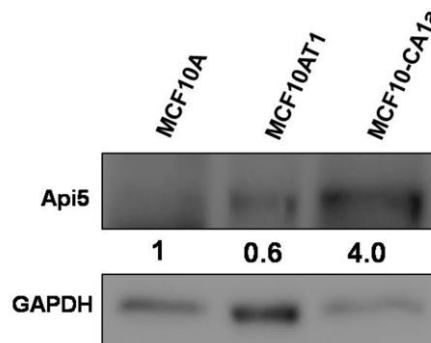


Figure 4: Api5 levels across cell lines belonging to MCF10A series. Cell lines belonging to MCF10A series were lysed and analyzed for Api5 levels.

Generation of a stable cell line of MCF10A over-expressing Api5

Lentiviral vector containing Api5 (mCherry-CSII-EF-MCS Api5) was prepared by cloning Api5 into mCherry-CSII-EF-MCS vector. This plasmid along with its packaging plasmids pCMV-VSV-G-RSV-Rev and pCAG-HIVgp were transfected into HEK 293T cells using calcium phosphate method. The collected viral supernatant was concentrated using Ultra centrifuge. As per the protocol of MOI determination, HEK 293T cells were seeded and different volumes of viral solution was used to transduce them (Figure 5). MOI for the viral solution was determined as shown below:

$$\text{MOI} = \frac{\text{Volume of viral supernatant required (ml)} \times \text{Titre (TU/ml)}}{\text{Target number of cells to be infected}}$$

Preferred MOI is 6.

$$6 = \frac{Z \times 1323 \times 10^3}{2 \times 10^5 \text{ (we plate this conc.)}}$$

Where z is the volume of viral supernatant required.

$$\mathbf{Z = 0.9 \text{ ml (approx)}}$$

0.9 ml of viral particles will be used to transduce **2 X 10⁵** cells.

MCF10A cells were then transduced with required amount of viral solution. mCherry positive cells were FACS sorted (Figure 6). Thus, Api5-MCF10A cell line was prepared.

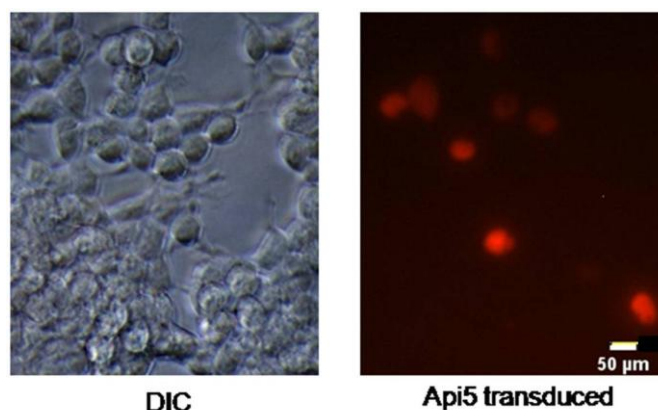


Figure 5: Representative image of transduced HEK 293T cells. HEK 293T was transduced by using different volumes of viral particles to determine MOI. Shown here is the representative image of transduced HEK 293T cells. The detailed protocol for MOI calculations is mentioned in methods section. Image was taken at 20X magnification.

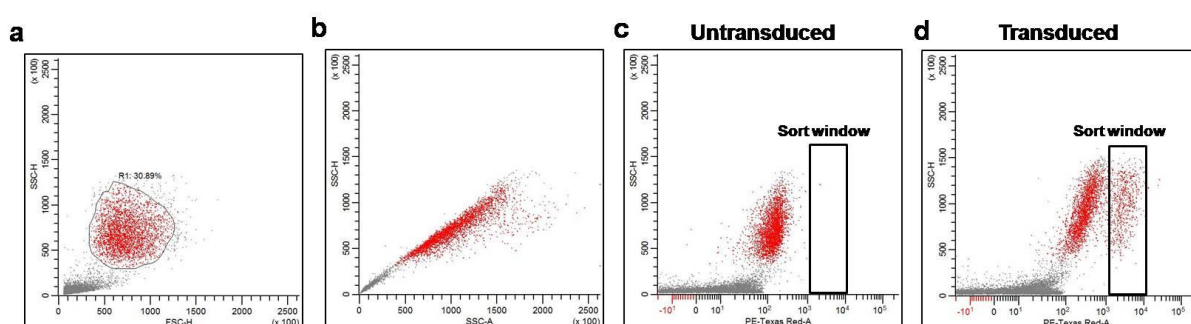


Figure 6: Sorting of Api5-MCF10A cells fluorescing mCherry. Data was analyzed using WinList version 8.0 software. (a) Live cells were segregated using SSC-height and FSC-height parameters. (b) SSC-area and SSC-height parameters were used to exclude cellular aggregates. (c) Untransduced cells as control. (d) Sorting window has been set for collecting Api5-MCF10A cells with desired levels of mCherry fluorescence.

We evaluated ectopically expressed Api5 levels using western blotting (Figure 7) and observed that the levels of exogenous Api5 is 4.5 times more than that of MCF10A cells.

There was no observable difference in the cellular morphologies of Api5-MCF10A and MCF10A cells grown as 2D cultures (Figure 8a). However, Api5-MCF10A cells showed morphological differences when grown as 3D cultures. The overall morphology of Api5-MCF10A acini was abnormal and appeared to be larger in size than that of MCF10A acini (Figure 8b).

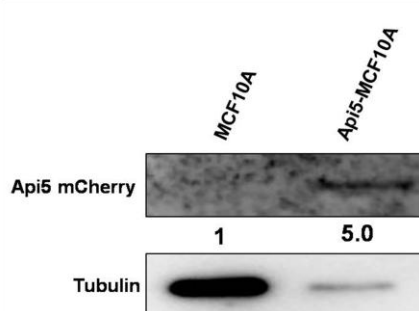


Figure 7: Api5 levels in Api5-MCF10A. MCF10A and Api5-MCF10A cells were lysed, analyzed for ectopically expressed Api5 levels.

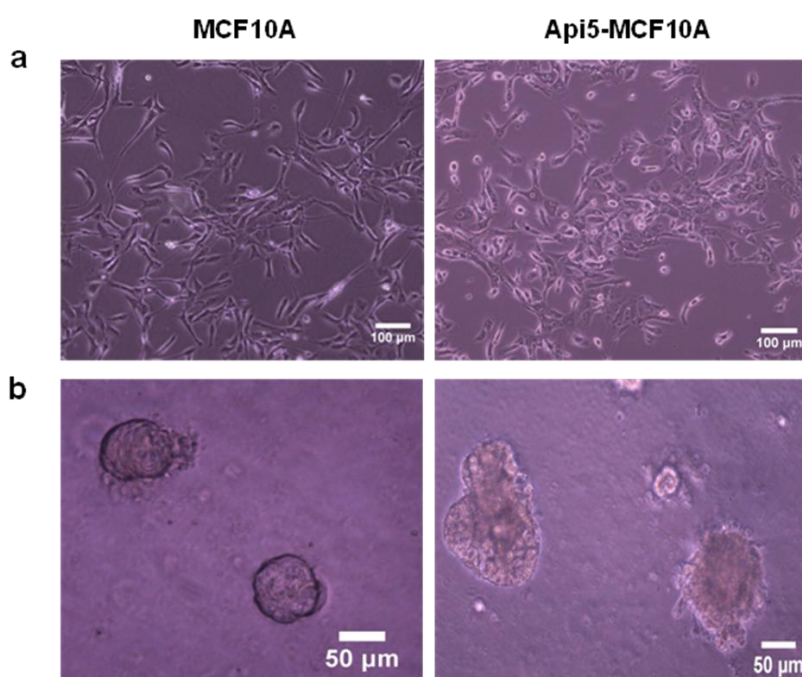


Figure 8: Morphological differences between MCF10A and Api5-MCF10A cells. Phase contrast images shown here are captured using Nikon microscope. (a) Api5 over-expression did not affect the morphology of MCF10A cells grown as 2D cultures. Images were taken at 10X magnification. However, (b) when MCF10A and Api5-MCF10A cells were grown on Matrigel[®] as '3D on top' cultures, Api5-MCF10A acini forms abnormal structures compared to that MCF10A acini. Api5-MCF10A acini also appear to be larger in size compared to MCF10A acini. Images were taken at 20X magnification.

Api5 over-expression resulted in increase in acinar size with enhanced cellular proliferation

MCF10A and Api5-MCF10A cells were grown on Matrigel® for 16 days. After 16 days, the cultures were fixed and immunostained for various markers.

Morphometric analysis of acini formed by Api5-MCF10A and MCF10A cells revealed that volume and surface area of the acini formed by Api5-MCF10A cells was significantly higher compared to acini formed by MCF10A cells (Figure **9a** and **9b**).

Further it was also observed that number of cells in Api5-MCF10A acini was significantly higher than that of MCF10A acini (Figure **10**).

To ascertain whether the increase in number of cells was due to enhanced cellular proliferation, Api5-MCF10A acini were immunostained for Ki67 (a proliferation marker). Based on the Ki67 staining, we inferred that by day 16, most of MCF10A acini formed growth arrested spheroids while Api5-MCF10A acini continued to proliferate (Figure **11a**). Acini with more than 6 Ki67 positive cells were considered to show enhanced proliferation (Wu and Gallo, 2013). We observed that 52% of Api5-MCF10A acini showed enhanced proliferation compared to only 2% of MCF10A acini (Figure **11b**).

Further analysis of the 3D spheroids revealed that most of the MCF10A cells formed acini with hollow lumen, while only 34% of the Api5-MCF10A acini formed hollow lumen. Moreover, the remaining 76% of Api5-MCF10A acini did not show a clear lumen phenotype (Figure **12a** and **12b**). On further analysis of these Api5-MCF10A acini, 41% of the acini showed positive staining for Ki67 in the lumen (Figure **11c**), suggesting that cells in the lumen have the ability to proliferate. However, we also observed that a few of these acini showed partial clearance of lumen. This may imply that there may be a delay or complete evasion of apoptosis during lumen formation, which will be studied by immunostaining for Cleaved caspase3, a marker for apoptosis across the time of morphogenesis and maintenance (> Day 16).

Taken together, data indicates that Api5 over-expression enhanced cellular proliferation resulting in increase in acinar size with no significant change in nuclear morphometry.

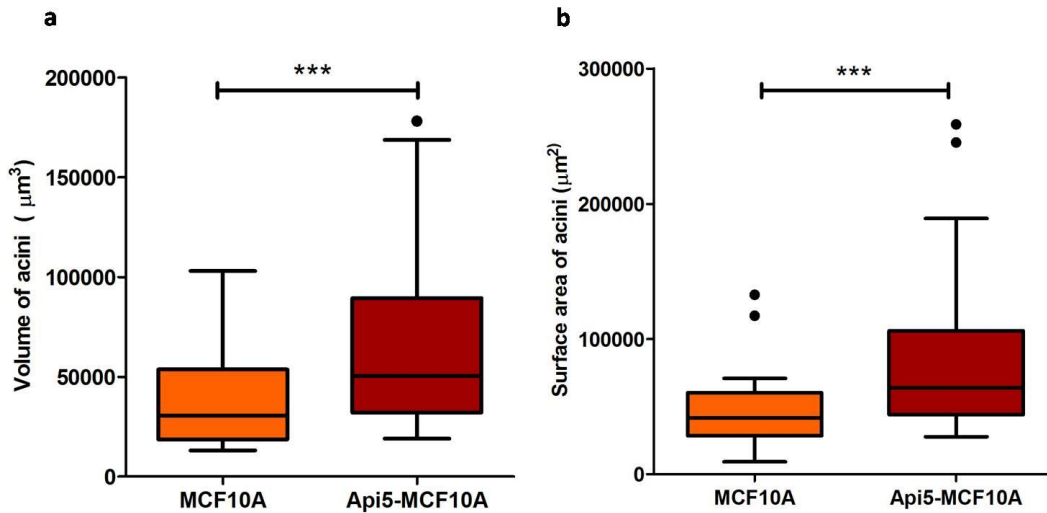


Figure 9: Over-expression of Api5 leads to increase in size of the acini.

MCF10A and Api5-MCF10A cells grown on Matrigel[®] for 16 days were fixed and stained for Phalloidin (marker for actin) and Hoechst 33342. The acini were then imaged using Zeiss LSM 710 laser scanning confocal microscope (Zeiss, GmbH) using 63X objective. (a) Volume of acini and (b) Surface area of acini was quantified using Huygens Professional Software and represented as a box plot. N=60, number of acini imaged per cell type from at least three independent experiments. Statistical analysis was performed using Mann Whitney test; *** p<0.0001 indicates significant differences between MCF10A acini and Api5-MCF10A acini.

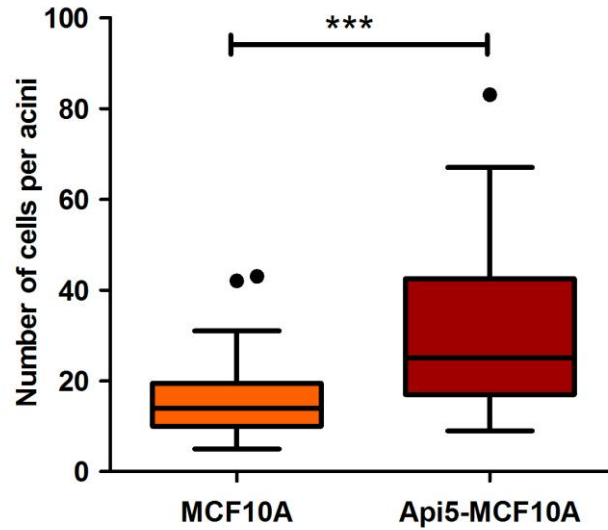


Figure 10: Api5 over-expression leads to increase in number of cells per acini. MCF10A and Api5-MCF10A cells, grown on Matrigel[®] for 16 days were fixed and stained with Hoechst 33342 (dye used to stain DNA). The acini were then imaged using Zeiss LSM 710 laser scanning confocal microscope (Zeiss, GmbH). Morphometric analysis of these acini was performed using Huygens Professional Software. Number of cells per acini was quantified, and represented as a box plot. N=60, number of acini imaged per cell type combined from at least three independent experiments. Statistical analysis was performed using Mann Whitney test; *** p<0.0001 indicates significant difference between MCF10A acini and Api5-MCF10A acini.

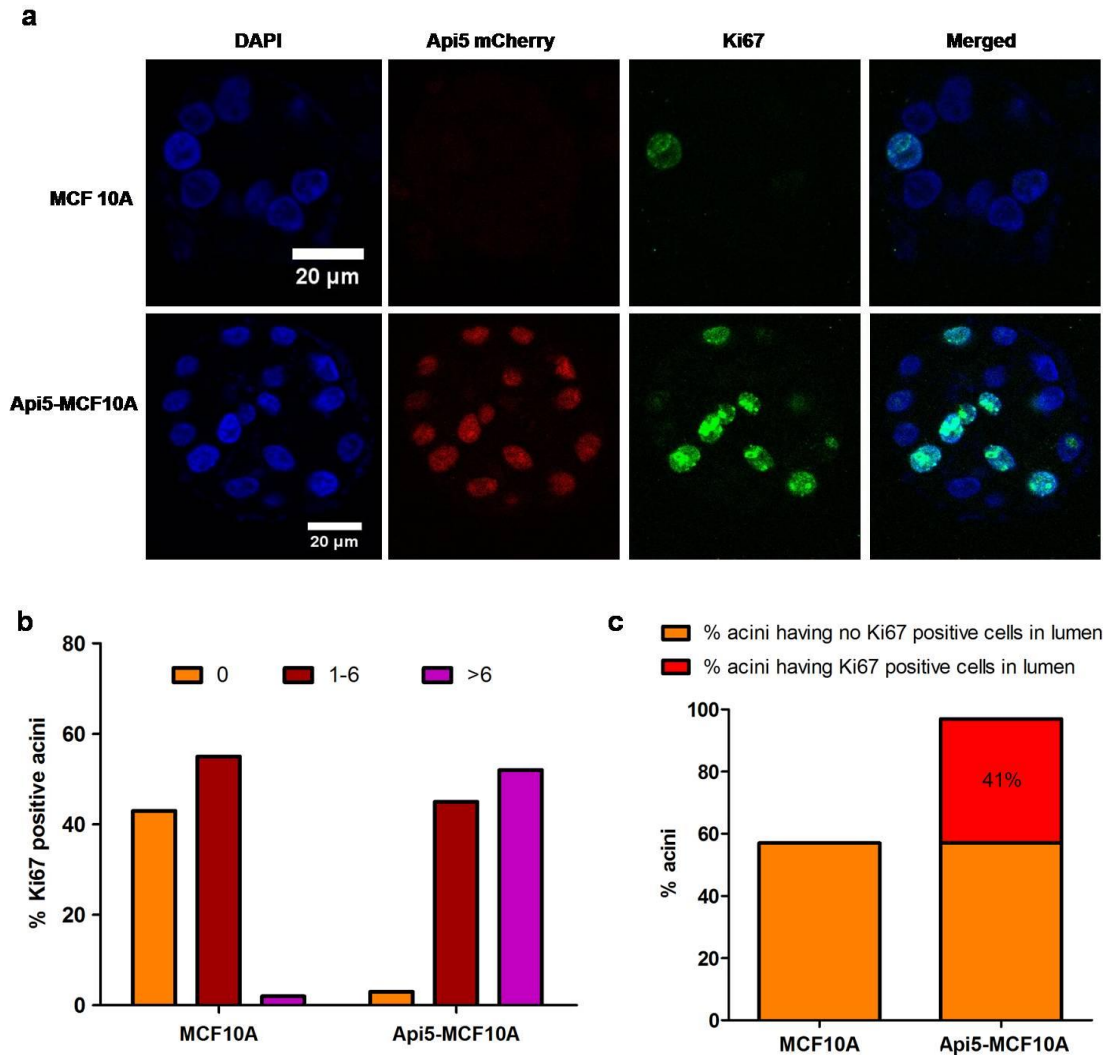


Figure 11: Api5 over-expression results in enhanced proliferation. 3D cultures of MCF10A cells and Api5-MCF10A cells grown on Matrigel[®] were fixed and immunostained for Ki67 (*green*), proliferation marker and Hoechst 33342 (*blue*). The acini were then imaged using Zeiss LSM 710 laser scanning confocal microscope (Zeiss, GmbH) using 63X objective. (a) Representative images of Api5-MCF10A acini and MCF10A acini showing Ki67 positive cells (b) Images were quantified for number of acini showing no Ki67 positive cells, 1 to 6 Ki67 positive cells or more than 6 Ki67 positive cells. (c) Images were quantified for presence of Ki67 positive cells in the lumen and represented as bar graphs. Results shown here were analyzed from 44 acini imaged per cell type combined from two independent experiments.

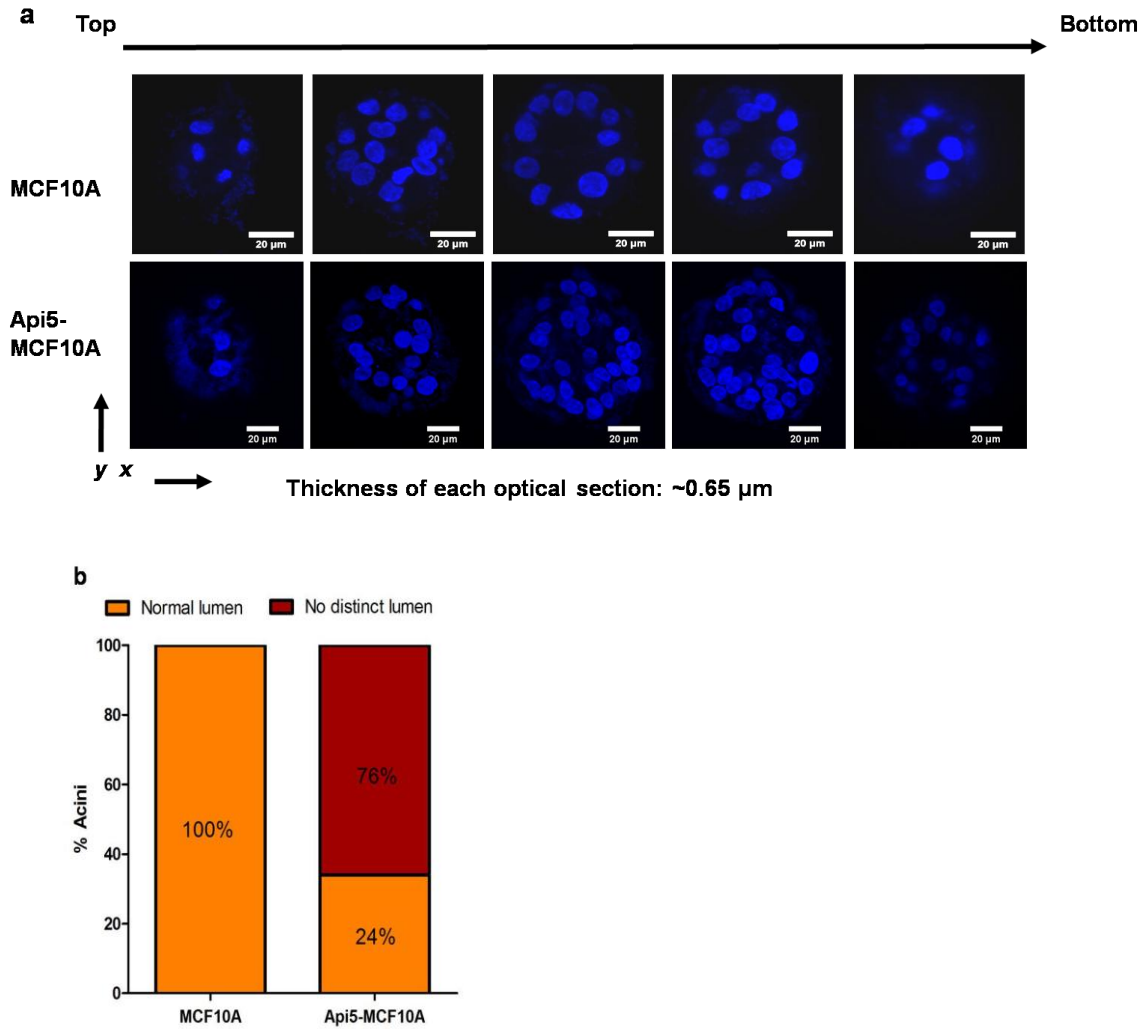


Figure 12: Api5-MCF10A cells form acini with partially cleared lumen.

MCF10A cells and Api5-MCF10A cells were grown as 3D ‘on top’ cultures. The acini were cultured for 16 days and then were immunostained for Hoechst 33342 (*blue*). Immunofluorescence images of 3D cultures were captured using Zeiss LSM 710 laser scanning confocal microscope (Zeiss, GmbH) using 63X oil objective. (a) Optical sections of acini from top to bottom. **Upper panel:** MCF10A acini showing single layer of cells surrounding the hollow lumen while **lower panel:** Api5-MCF10A acini showing partially filled lumen. Distance between each optical section was $0.65 \mu\text{m}$. (b) Percent of acini failed to form with distinct lumen was quantified and represented as bar graphs. $N=80$; number of acini quantified from two independent experiments.

Increase in nuclear size is another morphological feature observed in transformed cells (Zink et al., 2004). On analysis of the nuclear morphometry of Api5-MCF10A and MCF10A cells in the acini, it was observed that elevated levels of Api5 in Api5-MCF10A acini did not significantly affect both nuclear volume and nuclear surface area compared to MCF10A acini (Figure 13a and 13b).

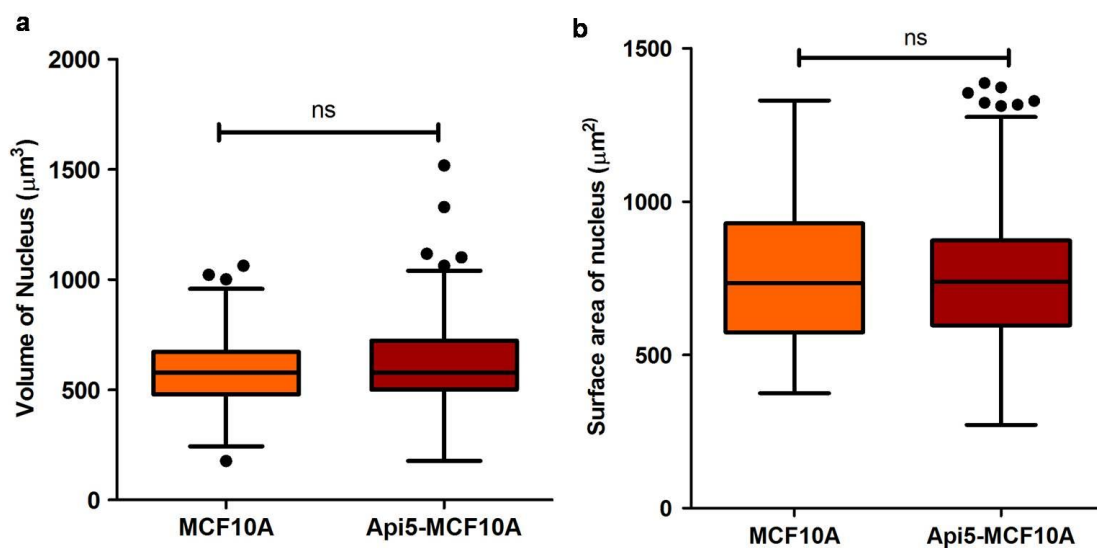


Figure 13: Api5 over-expression does not affect nuclear size. Day 16 3D cultures of MCF10A cells and Api5-MCF10A cells were fixed and nuclei were stained with Hoechst 33342. The acini were then imaged using Zeiss LSM 710 laser scanning confocal microscope (Zeiss, GmbH) using 63X objective. Morphometric analysis of these acini was performed using Huygens Professional Software. (a) Volume of nucleus and (b) Surface area of nucleus was quantified, and represented as a box plot. N=125, number of nuclei quantified per cell type from two independent experiments. Statistical analysis was performed using Mann Whitney test; *** $p < 0.0001$ indicates significant differences between MCF10A acini and Api5-MCF10A acini.

Api5 over-expression caused disruption of Apico-Basal polarity

Loss of polarity is one of the most commonly observed phenotype in epithelial cancers. Establishment of polarity can be studied using 3D cultures of MCF10A cells. We investigated the effect of Api5 over-expression on apico-basal polarity in the 3D acini. Immunostaining for GM130, a marker for Golgi apparatus was used as an apical polarity marker. Confocal analysis revealed that Api5 over-expression in MCF10A acini resulted in mislocalization of GM130 (Figure **14a**). On quantitative analysis, we found that 97% of Api5-MCF10A acini showed either basal or lateral localization of GM130 while MCF10A acini showed apical localization (region facing the lumen) (Figure **14b**).

α 6-Integrin, a basal region marker was used to examine integrity of basal polarity. Api5 over-expression in MCF10A acini resulted in loss or discontinuous staining of α 6-Integrin at the basal surface (Figure **15a**). In addition, Api5 over-expressed MCF10A acini also showed diffused staining of α 6-integrin at the basal region. Overall, 69% of the analyzed Api5-MCF10A acini showed loss of α 6-Integrin while 19% of the Api5-MCF10A acini showed diffused staining at the basal region (Figure **15b**).

We also investigated integrity of another basal polarity marker, Laminin V, a basement membrane protein. Our preliminary experiments showed that unlike the continuous staining of Laminin V in MCF10A (Figure **16: upper panel**), Api5-MCF10A acini showed loss or discontinuous staining of Laminin V at the basal region. In addition, we also noticed that Laminin V was mislocalized to inner regions of Api5-MCF10A acini (Figure **16: lower panel**).

These data together suggest that Api5 up-regulation in MCF10A cells disrupted apico-basal polarity.

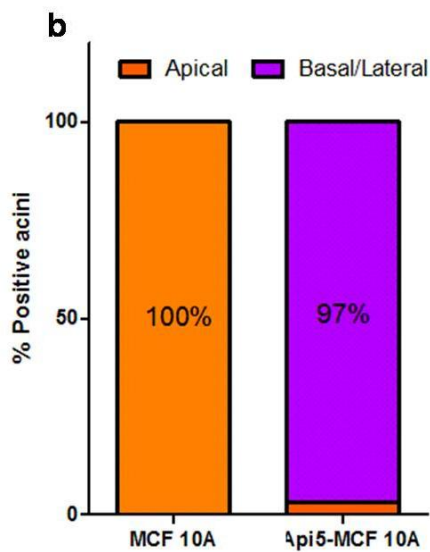
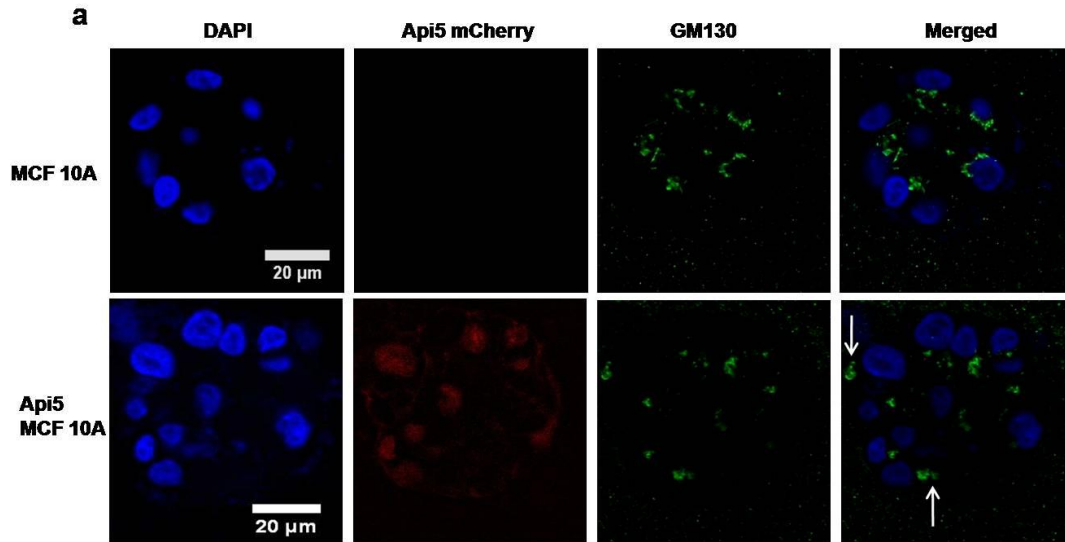


Figure 14: Api5 over-expression disrupts apical polarity. MCF10A and Api5-MCF10A cells were cultured for 16 days on Matrigel[®], immunostained for GM130 (green), Golgi body marker and images were captured using Zeiss LSM 710 laser scanning confocal microscope (Zeiss, GmbH) using 63X objective. (a) Representative images of **upper panel**: MCF10A acini retain apical localization of Golgi body while **lower panel**: Api5-MCF10A acini showing baso-lateral localization of GM130 (b) Images were quantified as percentage of acini showing mislocalization of GM130 and represented as bar graphs. N=43, number of acini quantified per cell type from two independent experiments.

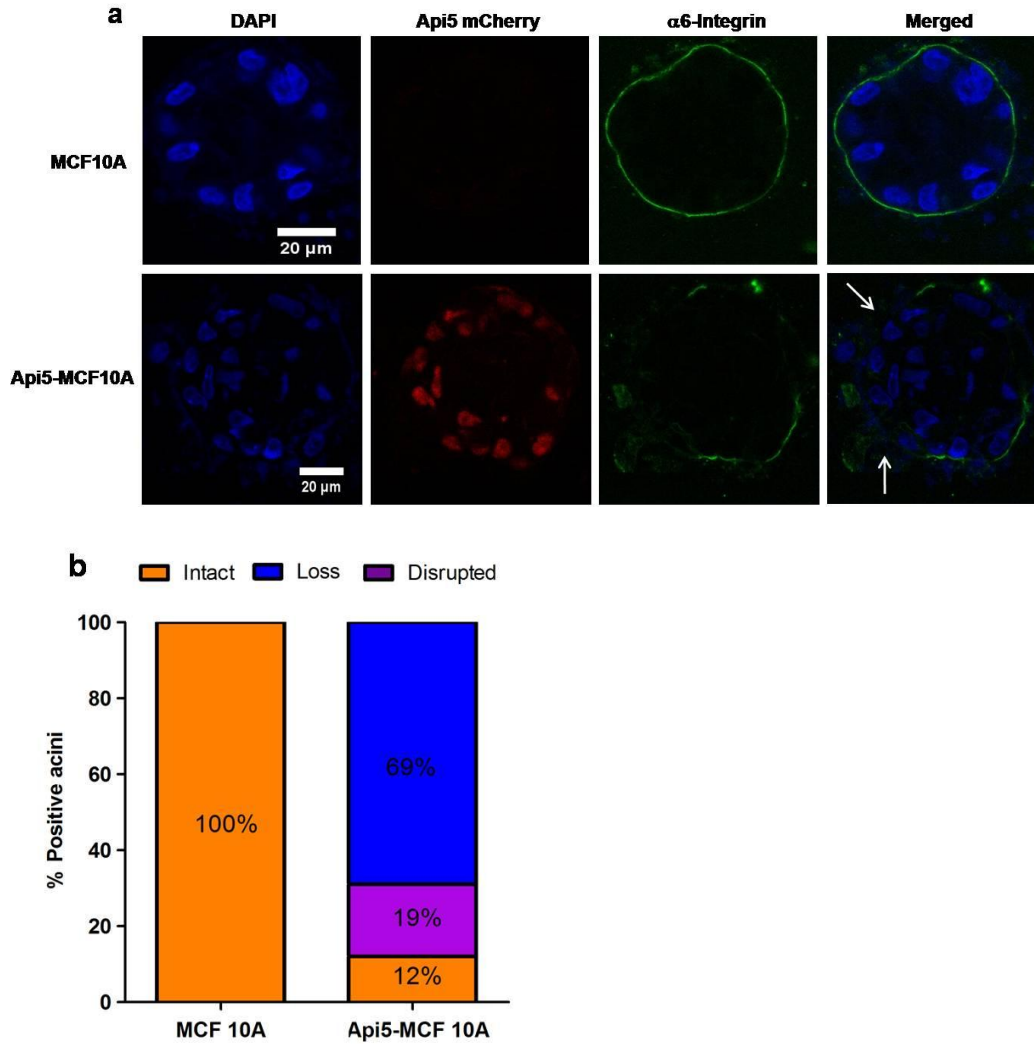


Figure 15: Api5 over-expression results in loss of $\alpha 6$ -Integrin. MCF10A and Api5-MCF10A cells were cultured for 16 days on Matrigel[®], immunostained for $\alpha 6$ -Integrin (*green*), basal region marker and images were captured using Zeiss LSM 710 laser scanning confocal microscope (Zeiss, GmbH) using 63X objective. (a) Representative images of **upper panel**: MCF10A acini with continuous staining of $\alpha 6$ -Integrin while **lower panel**: Api5-MCF10A acini showing loss/discontinuous/diffused $\alpha 6$ -Integrin staining. (b) Images were quantified as percentage of acini showing loss/discontinuous/diffused staining of $\alpha 6$ -Integrin and represented as bar graphs. N=51, number of acini quantified per cell type from two independent experiments.

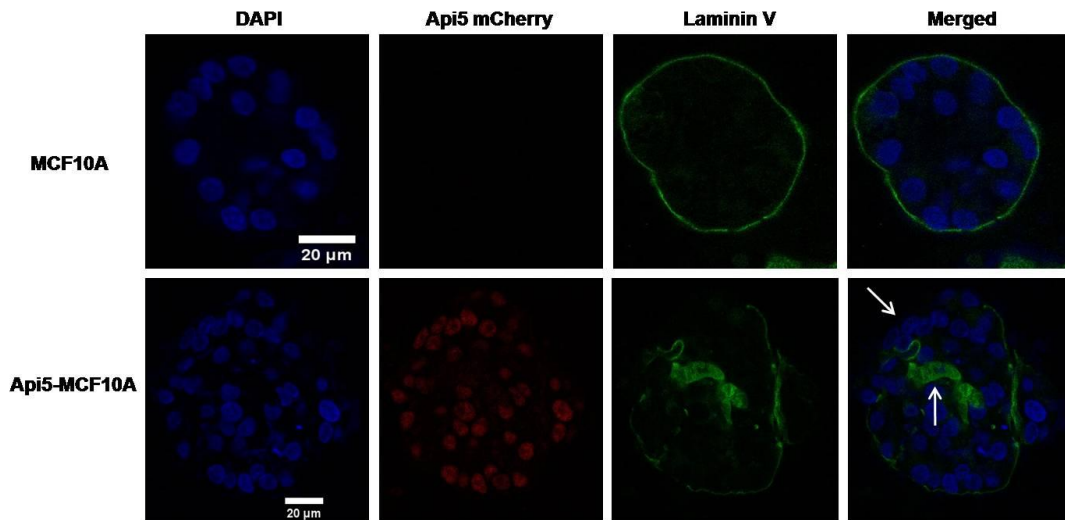


Figure 16: Api5 over-expression results in loss of Laminin V.

MCF10A and Api5-MCF10A cells were cultured for 16 days on Matrigel[®], immunostained for Laminin V (*green*), basement membrane protein and images were captured using Zeiss LSM 710 laser scanning confocal microscope (Zeiss, GmbH) using 63X objective. Representative images of **upper panel**: MCF10A acini showing continuous staining of Laminin V at the basal region while **lower panel**: Api5-MCF10A acini showing loss and/or mislocalized Laminin V staining.

Api5 over-expression disrupted cell-cell junctions.

Loss of cell-cell junctions is known to be associated with loss of polarity. Hence, we investigated the effect of Api5 over-expression on cell-cell junctions. To address this, immunostaining of E-Cadherin and β -Catenin was performed. Our analysis revealed that Api5 over-expression resulted in loss and/or aberrant expression of E-Cadherin (Figure **17a**). On quantification, we observed that 60% of Api5-MCF10A acini showed loss of E-Cadherin while MCF10A acini showed intact staining (Figure **17b**). Preliminary experiments for the analysis of β -Catenin expression revealed that Api5 over-expression resulted in loss of β -Catenin expression in the acini (Figure **18**).

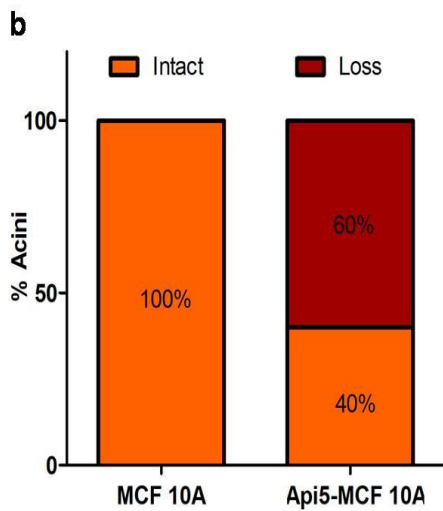
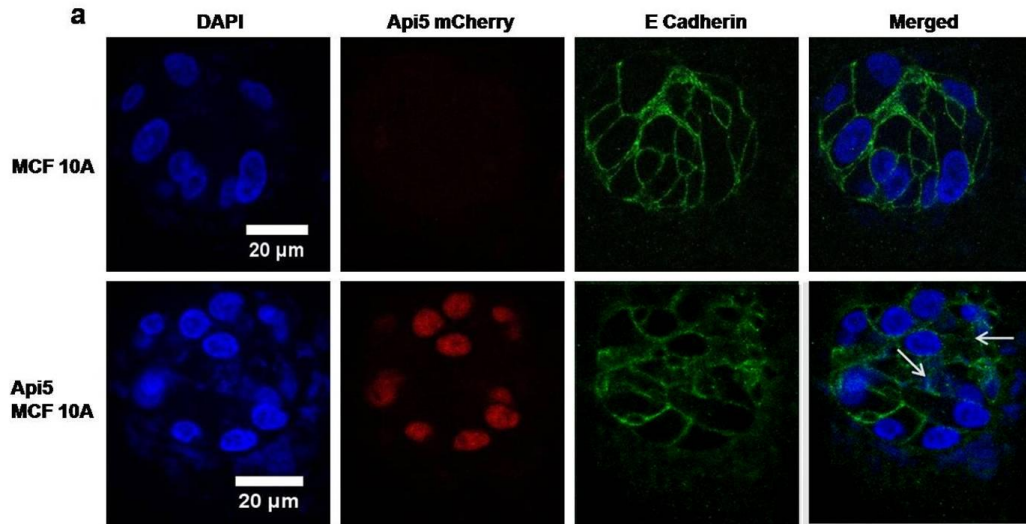


Figure 17: Api5 over-expression leads to loss of E Cadherin, cell-cell junction protein. MCF10A and Api5-MCF10A cells were cultured for 16 days on Matrigel[®], immunostained for E Cadherin (*green*), epithelial cell-cell junction protein and images were captured using Zeiss LSM 710 laser scanning confocal microscope (Zeiss, GmbH) using 63X objective. (a) Representative images of **upper panel**: MCF10A acini showing intact staining of E-Cadherin while **lower panel**: Api5-MCF10A acini showing aberrant expression of E-Cadherin. (b) Images were quantified as percentage of Api5-MCF10A acini showing aberrant expression of E-Cadherin. N=33, number of acini quantified per cell type from one experiment.

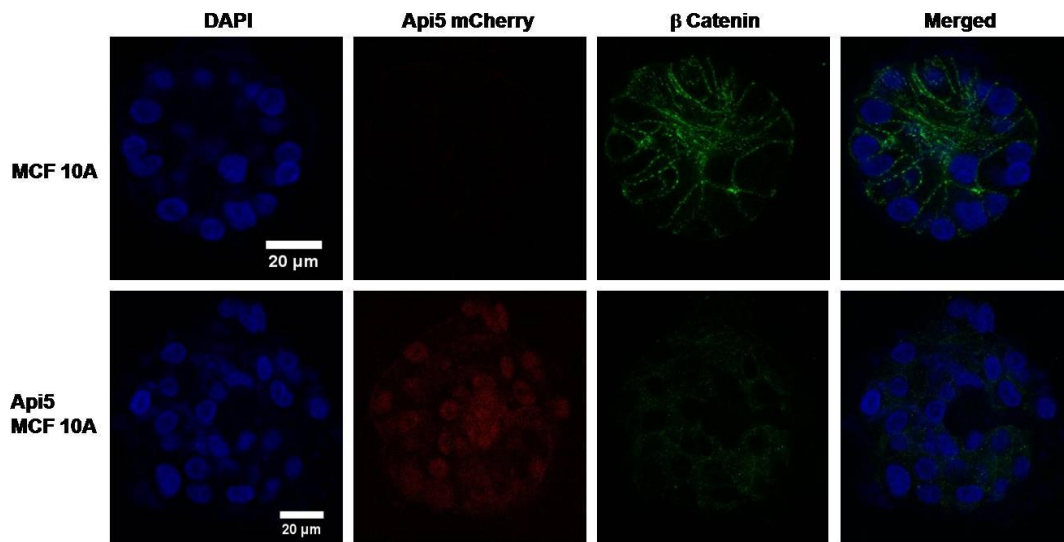


Figure 18: Api5 over-expression leads to loss of β -Catenin, cell-cell junction protein. MCF10A and Api5-MCF10A cells were cultured for 16 days on Matrigel[®], immunostained for β -Catenin (*green*), epithelial cell-cell junction protein and images were captured using Zeiss LSM 710 laser scanning confocal microscope (Zeiss, GmbH) using 63X objective. (a) Representative images of **upper panel:** MCF10A acini showing intact staining of β -Catenin while **lower panel:** Api5-MCF10A acini showing loss of β -Catenin.

Api5 over-expression induced up-regulation of Vimentin, an Epithelial to Mesenchymal transition (EMT) marker.

Disruption of cell-cell junctions is not only associated with disruption of polarity but is also indicative of an EMT-like phenotype. EMT is one of the early events in the process of invasion in epithelial cancers. Also, considering the strong association of Api5 with invasion of cancer cells, we investigated whether Api5 over-expression induced EMT-like phenotype in MCF10A cells. In this study, Vimentin, an intermediate filament protein, which is known to be up-regulated in mesenchymal cells, was used as an EMT marker. An up-regulation of Vimentin was observed in Api5-MCF10A as compared to control MCF10A acini (Figure **19a**). On quantification, 89% of Api5-MCF10A acini showed up-regulation of Vimentin while a basal level of staining was observed in MCF10A acini (Figure **19a** and **19b**).

EMT-like phenotype observed in Api5-MCF10A acini will be further confirmed using other EMT markers including fibronectin, Snail and Slug by immunoblotting as well as quantitative PCR.

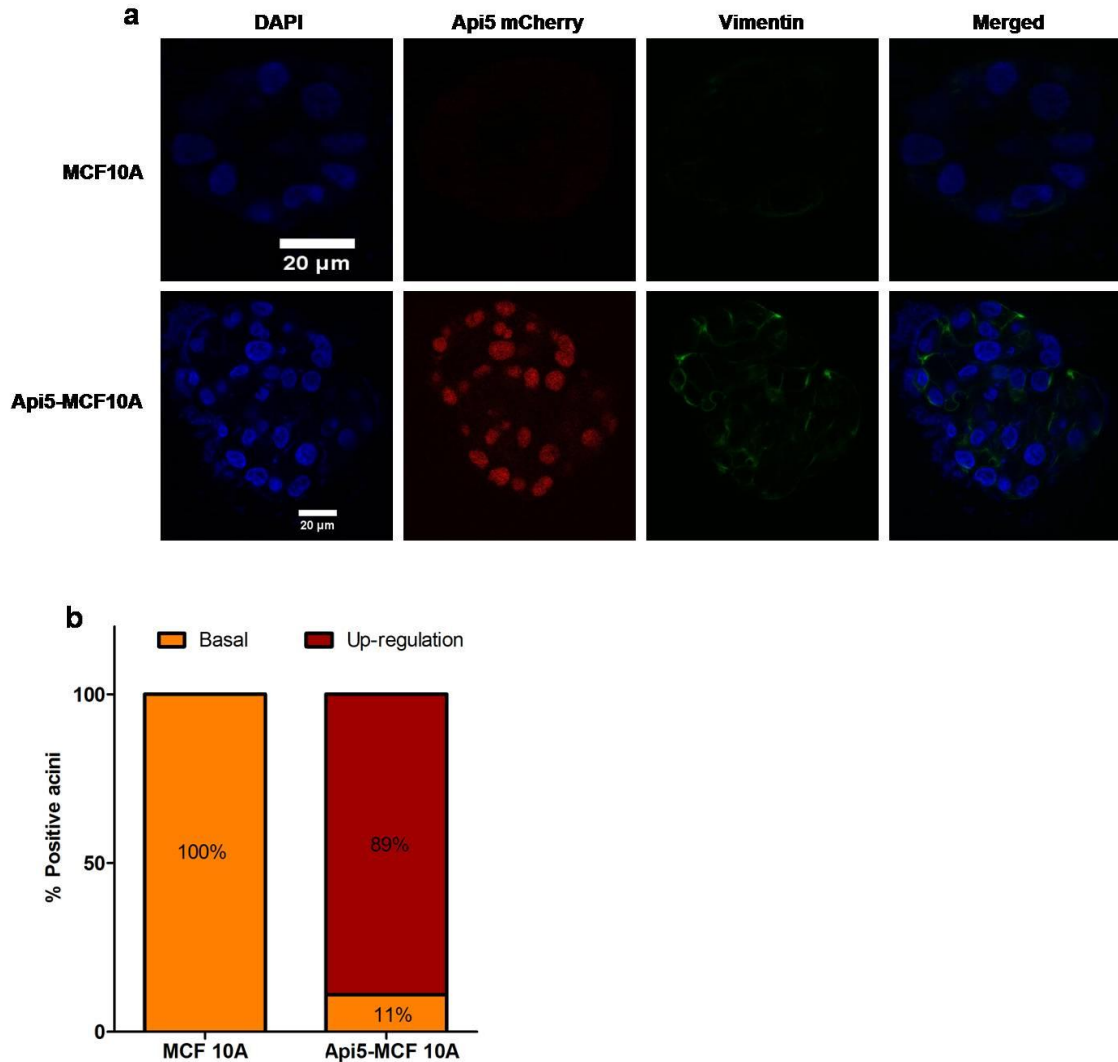


Figure 19: Api5 over-expression results in up-regulation of Vimentin, an EMT marker. MCF10A and Api5-MCF10A cells were cultured for 16 days on Matrigel[®], immunostained for Vimentin (*green*), mesenchymal marker and images were captured using Zeiss LSM 710 laser scanning confocal microscope (Zeiss, GmbH) using 63X objective. (a) Representative images of **upper panel:** MCF10A acini showing basal staining of Vimentin while **lower panel:** Api5-MCF10A acini showing up-regulated Vimentin expression. (b) Images were quantified as percentage of Api5-MCF10A acini showing up-regulated Vimentin expression compared to that of MCF10A acini. N=30, number of acini quantified per cell type from two independent experiments.

Api5-MCF10A cells seeded on Collagen-Matrigel[®] failed to form acini.

Apart from an up-regulation of Vimentin, we also observed the presence of “protrusion-like” or “bulb-like structures” in 60% of Api5-MCF10A acini (Figure **20a** and **20b**). Such phenotypes are indicative of either migratory or invasive behavior. Therefore, a Collagen-Matrigel invasion assay was performed to investigate the invasive potential of Api5-MCF10A cells. Interestingly, we observed that Api5-MCF10A cells seeded on collagen-Matrigel[®] failed to form acini and grew as sheets of cells. This phenotype indicated that altering the matrix affected the morphogenesis of Api5-MCF10A cells.

Further, to confirm the invasive potential of these cells other 3D invasion assays (collagen plug assay, “cell sandwiching” assay) will be performed.

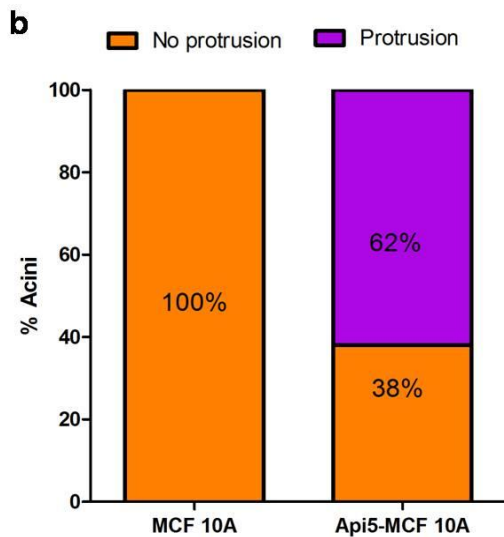
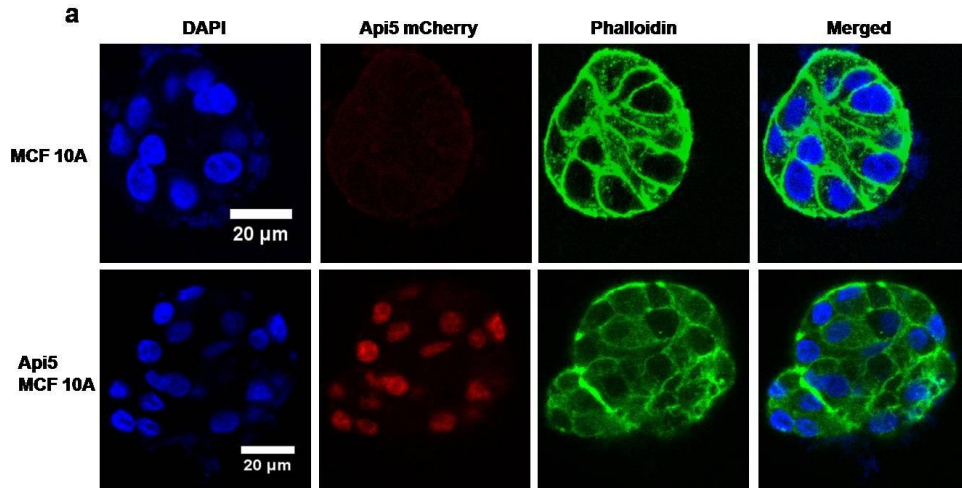


Figure 20: Api5 over-expression results in formation of migratory or invasive 3D structures. 3D cultures of MCF10A cells and Api5-MCF10A cells grown on Matrigel[®] were fixed and stained for Phalloidin (*green*) and Hoechst 33342 (*blue*) and were imaged using Zeiss LSM 710 laser scanning confocal microscope (Zeiss, GmbH) with 63X objective. Scale bar: 20 μm. (a) Representative image of **upper panel**: MCF10A acini showing a spherical morphology **lower panel**: protrusion like or bulb like structures formed in Api5-MCF10A acini. (b) Images were quantified for presence of protrusion like or bulb like structures and was represented as bar graphs. N=60, number of acini quantified per cell type combined from two independent experiments.

Discussion:

Api5 has been found to be up-regulated in various cancers (Noh et al., 2014; Sasaki et al., 2001; Song et al., 2014) and has been implicated as a potential oncogene. However its role in breast cancer has not been studied. To our knowledge, this is the first study to investigate and understand the role of Api5 in breast tumorigenesis. Our preliminary data indicated the presence of high levels of Api5 in MCF10-CA1a, as compared to MCF10A. MCF10-CA1a is a malignant invasive cell line belonging to MCF10A series. This data along with the reports from Radhakrishnan (Ramdas et al., 2011) and Berns labs (Jansen et al., 2005) indicated that high levels of Api5 might play a role in breast cancer. This prompted us to investigate the role of Api5 in breast epithelial cell transformation using 3D cultures of breast acini. 3D cultures of breast epithelial cells have been found to be an ideal system to study the role of a single gene or a small subset of genes in tumor initiation or tumor promotion (Mills et al., 2004; Reginato et al., 2005). Moreover, the spheroids formed in these cultures recapitulate the *in vivo* scenario to a greater extent (Vidi et al., 2013) thus making them the most suitable model system to study the role of several oncogenes and tumor suppressors.

3D cultures of transformed epithelial cells are known to model many features which are characteristic of epithelial cancers such as de-regulation of apico-basal polarity, luminal filling, and hyperproliferation (Debnath and Brugge, 2005). In addition to these, change in nuclear morphology has been observed in many cancers and its morphometry is considered as an important diagnostic and predictive marker for cancers (Baak et al., 1985; van Diest and Baak, 1991).

Using this platform, we investigated the role of Api5 in transformation. Api5 was over-expressed in MCF10A cells to attain a level comparable to that of MCF10-CA1a. These cells when grown on ECM gave rise to spheroids having characteristics of epithelial cancers. Mis-localization of GM130 along with loss of $\alpha 6$ integrin and Laminin V indicated disruption of apico-basal polarity. The phenotype observed with regards to GM130 and Laminin V was similar to that reported by Muthuswamy's group (Zhan et al., 2006). In addition to this, it has also been observed that cells in their invasive stage lose their cell-cell junctions,

break the basement membrane so as to invade the ECM and migrate into the nearby tissue. Thus loss of $\alpha 6$ -Integrin and laminin V observed in Api5-MCF10A acini indicated decreased or loss of interaction with ECM resulting in abrogation of signaling from ECM, thereby disrupting apico-basal polarity. The appearance of a discontinuous basement membrane upon Api5 over-expression coupled with loss of cell-cell junctions implied a possible invasive phenotype induced by Api5 in non-transformed breast epithelial cells.

Loss of the junctional proteins has been reported to be required for the induction of EMT (Moreno-Bueno et al., 2008), an early event in the process of invasion (Wu and Zhou, 2008). Furthermore, loss of E-Cadherin was shown to promote invasion through up-regulation of EMT inducers (Larue and Bellacosa, 2005). In addition to this, FGF2, which has been shown to be up-regulated upon Api5 up-regulation (Krejci et al., 2007; Noh et al., 2014) has been shown to down-regulate E-Cadherin in ovarian cancer cells (Lau et al., 2013) as well as induce EMT in urothelial carcinoma cell lines (Tomlinson et al., 2012). Furthermore previously published reports suggested that Api5 played a role in cancer cell invasion (Kim et al., 2000; Song et al., 2014). Considering the above mentioned reports we investigated whether Api5 can induce EMT in MCF10A, using Vimentin, whose levels are known to be elevated in mesenchymal cells (Sarrio et al., 2008). Api5 over-expression in MCF10A resulted in up-regulation of Vimentin. Supporting this data, we also observed that Api5-MCF10A acini form “protrusion-like” or “bulb-like” structures, which is an indication of either migratory or invasive phenotypes. Thus, loss of cell-cell junctions as well as up-regulation of Vimentin and presence of protrusion-like or bulb-like structures suggested that Api5 over-expression may induce invasive like phenotypes in MECs.

To confirm the possible invasive behavior of cells in Api5-MCF10A acini, Matrigel[®]: Collagen invasion assay was performed. The preliminary results showed that Api5-MCF10A cells failed to form acini and instead formed sheets of cells indicating failure of cells to differentiate on stiffened matrix thus further supporting the claim that Api5 over-expression has the potential to induce an invasive phenotype. 3D Matrigel[®]-collagen plug-invasion assays will be

performed to further validate the results. This will be supported by detailed investigations using other immunoblotting and quantitative PCR.

Increase in nuclear size is another morphological change displayed by transformed cells (Zink et al., 2004). However, in our study, there was no significant difference in the nuclear morphometry of Api5-MCF10A and MCF10A cells, implying that Api5 over expression did not affect nuclear morphology

Api5 over-expression in MCF10A cells also resulted in formation of large acini with increased number of cells and no distinct lumen. In addition to this there was an increase in number of Ki67 positive cells in the acini. A few acini also showed partial clearance of lumen with the luminal cells also staining positive for Ki67. These phenotypes mimic hyperproliferation and lumen filling which are key features seen in atypical hyperplasia and ductal carcinoma *in situ* (DCIS) (Debnath and Brugge, 2005; Reginato and Muthuswamy, 2006) as well as have been earlier reported and attributed to oncogene mediated “constitutive stimulation of proliferation and antiapoptotic activities” (Reginato et al., 2005). These phenotypes may be the consequence of the known well established function of Api5 of apoptosis inhibition through down-regulation of BIM as well as enhanced cellular proliferation through E2F1 mediated transcriptional activation of G1/S cell cycle genes (Garcia-Jove Navarro et al., 2013).

Taken together, the above-mentioned phenotypes observed in over-expressed Api5 MCF10A acini, suggested its possible role in breast tumorigenesis. However, the results presented here demand for further validation using biochemical techniques such as immunoblotting and quantitative PCR. Further investigations are required to delineate the pathway(s) involved in Api5-induced transformation, which may aid in the designing of novel therapeutics.

Future perspectives:

Taking into consideration the various phenotypes observed following over-expression of Api5 in MCF 10A cells grown as 3D breast acini, it is important to dissect out the molecular pathway(s) that may be de-regulated during the tumorigenesis process. Literature suggests a few pathways (summarized in

figure 21), which can be associated with the observed phenotypes. Following up on these pathways may aid in delineating the mechanisms involved. Cellular proliferation, a key phenotype observed in this study, may be attributed to the role of Api5 in enhancing the E2F1-mediated transcriptional activation of G1/S cell cycle genes (Garcia-Jove Navarro et al., 2013).

Previously published reports suggest Api5 activated ERK, which in turn resulted in transcriptional activation of AP-1 finally resulting in secretion of MMP9 (Song et al., 2014) to induce invasion. EMT like phenotype may be attributed to up-regulation of FGF2 by Api5, which in turn can activate down-stream signaling (Lau et al., 2013; Noh et al., 2014; Tomlinson et al., 2012). Considering all these reports it can be speculated that the invasive phenotype as well as the loss of cell-cell junctions observed in our study may be mediated through FGF2.

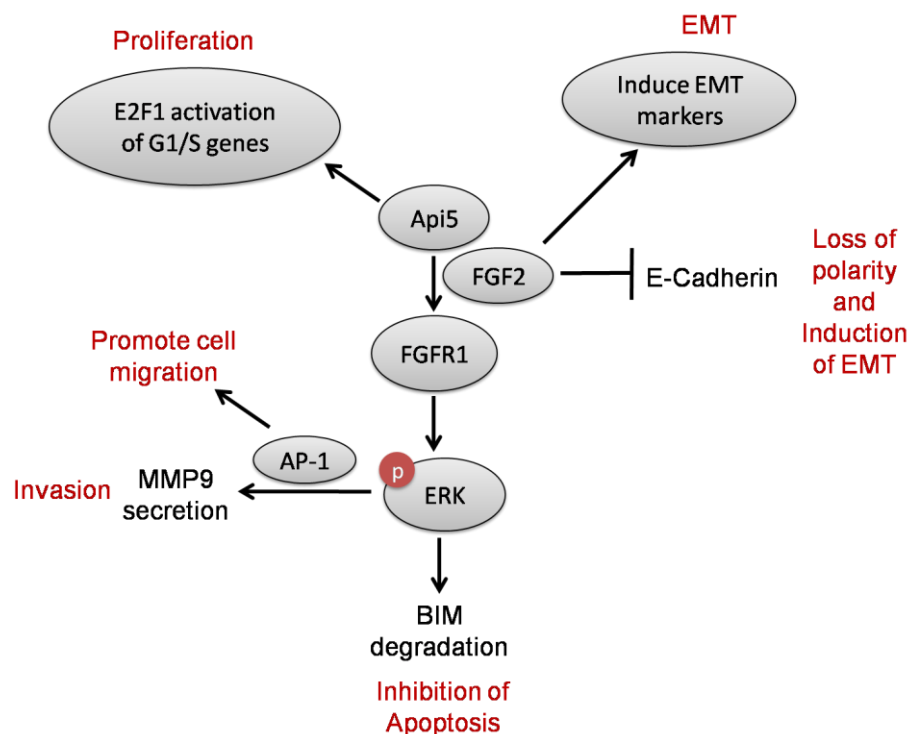


Figure 211: Suggested pathways that may be involved in observed phenotypes upon Api5 over-expression.

However, experiments have to be designed to prove these speculations made based on literature.

References:

- Baak, J.P., Van Dop, H., Kurver, P.H., and Hermans, J. (1985). The value of morphometry to classic prognosticators in breast cancer. *Cancer* 56, 374-382.
- Bissell, M.J., and Radisky, D. (2001). Putting tumours in context. *Nat Rev Cancer* 1, 46-54.
- Damiola, F., Pertesi, M., Oliver, J., Le Calvez-Kelm, F., Voegelé, C., Young, E.L., Robinot, N., Forey, N., Durand, G., Vallee, M.P., *et al.* (2014). Rare key functional domain missense substitutions in MRE11A, RAD50, and NBN contribute to breast cancer susceptibility: results from a Breast Cancer Family Registry case-control mutation-screening study. *Breast Cancer Res* 16, R58.
- Dawson, P.J., Wolman, S.R., Tait, L., Heppner, G.H., and Miller, F.R. (1996). MCF10AT: a model for the evolution of cancer from proliferative breast disease. *Am J Pathol* 148, 313-319.
- Debnath, J., and Brugge, J.S. (2005). Modelling glandular epithelial cancers in three-dimensional cultures. *Nat Rev Cancer* 5, 675-688.
- Ellis, M.J., Ding, L., Shen, D., Luo, J., Suman, V.J., Wallis, J.W., Van Tine, B.A., Hoog, J., Goiffon, R.J., Goldstein, T.C., *et al.* (2012). Whole-genome analysis informs breast cancer response to aromatase inhibition. *Nature* 486, 353-360.
- Garcia-Jove Navarro, M., Basset, C., Arcondeguy, T., Touriol, C., Perez, G., Prats, H., and Lacazette, E. (2013). Aip5 contributes to E2F1 control of the G1/S cell cycle phase transition. *PLoS One* 8, e71443.
- Guilford, P., Hopkins, J., Harraway, J., McLeod, M., McLeod, N., Harawira, P., Taite, H., Scoular, R., Miller, A., and Reeve, A.E. (1998). E-cadherin germline mutations in familial gastric cancer. *Nature* 392, 402-405.
- Han, B.G., Kim, K.H., Lee, S.J., Jeong, K.C., Cho, J.W., Noh, K.H., Kim, T.W., Kim, S.J., Yoon, H.J., Suh, S.W., *et al.* (2012). Helical repeat structure of apoptosis inhibitor 5 reveals protein-protein interaction modules. *J Biol Chem* 287, 10727-10737.
- Hemminki, A., Markie, D., Tomlinson, I., Avizienyte, E., Roth, S., Loukola, A., Bignell, G., Warren, W., Aminoff, M., Hoglund, P., *et al.* (1998). A serine/threonine kinase gene defective in Peutz-Jeghers syndrome. *Nature* 391, 184-187.
- Hill, V.K., Hesson, L.B., Dansranjavin, T., Dallol, A., Bieche, I., Vacher, S., Tommasi, S., Dobbins, T., Gentle, D., Euhus, D., *et al.* (2010). Identification of 5 novel genes methylated in breast and other epithelial cancers. *Mol Cancer* 9, 51.
- Jansen, M.P., Foekens, J.A., van Staveren, I.L., Dirkzwager-Kiel, M.M., Ritstier, K., Look, M.P., Meijer-van Gelder, M.E., Sieuwerts, A.M., Portengen, H.,

Dorssers, L.C., *et al.* (2005). Molecular classification of tamoxifen-resistant breast carcinomas by gene expression profiling. *J Clin Oncol* 23, 732-740.

Jenne, D.E., Reimann, H., Nezu, J., Friedel, W., Loff, S., Jeschke, R., Muller, O., Back, W., and Zimmer, M. (1998). Peutz-Jeghers syndrome is caused by mutations in a novel serine threonine kinase. *Nat Genet* 18, 38-43.

Kadota, M., Yang, H.H., Gomez, B., Sato, M., Clifford, R.J., Meerzaman, D., Dunn, B.K., Wakefield, L.M., and Lee, M.P. (2010). Delineating genetic alterations for tumor progression in the MCF10A series of breast cancer cell lines. *PLoS One* 5, e9201.

Khaled, W.T., Choon Lee, S., Stingl, J., Chen, X., Raza Ali, H., Rueda, O.M., Hadi, F., Wang, J., Yu, Y., Chin, S.F., *et al.* (2015). BCL11A is a triple-negative breast cancer gene with critical functions in stem and progenitor cells. *Nat Commun* 6, 5987.

Kim, J.W., Cho, H.S., Kim, J.H., Hur, S.Y., Kim, T.E., Lee, J.M., Kim, I.K., and Namkoong, S.E. (2000). AAC-11 overexpression induces invasion and protects cervical cancer cells from apoptosis. *Lab Invest* 80, 587-594.

Kim, P.J., Plescia, J., Clevers, H., Fearon, E.R., and Altieri, D.C. (2003). Survivin and molecular pathogenesis of colorectal cancer. *Lancet* 362, 205-209.

Klos, K.S., Warmka, J.K., Drachenberg, D.M., Chang, L., Luxton, G.W., Leung, C.T., Schwertfeger, K.L., and Wattenberg, E.V. (2014). Building bridges toward invasion: tumor promoter treatment induces a novel protein kinase C-dependent phenotype in MCF10A mammary cell acini. *PLoS One* 9, e90722.

Koci, L., Chlebova, K., Hyzdalova, M., Hofmanova, J., Jira, M., Kysela, P., Kozubik, A., Kala, Z., and Krejci, P. (2012). Apoptosis inhibitor 5 (API-5; AAC-11; FIF) is upregulated in human carcinomas *in vivo*. *Oncol Lett* 3, 913-916.

Krejci, P., Pejchalova, K., Rosenbloom, B.E., Rosenfelt, F.P., Tran, E.L., Laurell, H., and Wilcox, W.R. (2007). The antiapoptotic protein Api5 and its partner, high molecular weight FGF2, are up-regulated in B cell chronic lymphoid leukemia. *J Leukoc Biol* 82, 1363-1364.

Larue, L., and Bellacosa, A. (2005). Epithelial-mesenchymal transition in development and cancer: role of phosphatidylinositol 3' kinase/AKT pathways. *Oncogene* 24, 7443-7454.

Lau, M.T., So, W.K., and Leung, P.C. (2013). Fibroblast growth factor 2 induces E-cadherin down-regulation via PI3K/Akt/mTOR and MAPK/ERK signaling in ovarian cancer cells. *PLoS One* 8, e59083.

Lee, J.P., Chang, K.H., Han, J.H., and Ryu, H.S. (2005). Survivin, a novel anti-apoptosis inhibitor, expression in uterine cervical cancer and relationship with prognostic factors. *Int J Gynecol Cancer* 15, 113-119.

Ma, X.J., Salunga, R., Tuggle, J.T., Gaudet, J., Enright, E., McQuary, P., Payette, T., Pistone, M., Stecker, K., Zhang, B.M., *et al.* (2003). Gene expression profiles of human breast cancer progression. *Proc Natl Acad Sci U S A* 100, 5974-5979.

Malkin, D., Li, F.P., Strong, L.C., Fraumeni, J.F., Jr., Nelson, C.E., Kim, D.H., Kassel, J., Gryka, M.A., Bischoff, F.Z., Tainsky, M.A., *et al.* (1990). Germ line p53 mutations in a familial syndrome of breast cancer, sarcomas, and other neoplasms. *Science* 250, 1233-1238.

Meijers-Heijboer, H., van den Ouweland, A., Klijn, J., Wasielewski, M., de Snoo, A., Oldenburg, R., Hollestelle, A., Houben, M., Crepin, E., van Veghel-Plandsoen, M., *et al.* (2002). Low-penetrance susceptibility to breast cancer due to CHEK2(*)1100delC in noncarriers of BRCA1 or BRCA2 mutations. *Nat Genet* 31, 55-59.

Mills, K.R., Reginato, M., Debnath, J., Queenan, B., and Brugge, J.S. (2004). Tumor necrosis factor-related apoptosis-inducing ligand (TRAIL) is required for induction of autophagy during lumen formation in vitro. *Proc Natl Acad Sci U S A* 101, 3438-3443.

Moreno-Bueno, G., Portillo, F., and Cano, A. (2008). Transcriptional regulation of cell polarity in EMT and cancer. *Oncogene* 27, 6958-6969.

Morris, E.J., Michaud, W.A., Ji, J.Y., Moon, N.S., Rocco, J.W., and Dyson, N.J. (2006). Functional identification of Api5 as a suppressor of E2F-dependent apoptosis in vivo. *PLoS Genet* 2, e196.

Muthuswamy, S.K., Li, D., Lelievre, S., Bissell, M.J., and Brugge, J.S. (2001). ErbB2, but not ErbB1, reinitiates proliferation and induces luminal repopulation in epithelial acini. *Nat Cell Biol* 3, 785-792.

Nelen, M.R., van Staveren, W.C., Peeters, E.A., Hassel, M.B., Gorlin, R.J., Hamm, H., Lindboe, C.F., Fryns, J.P., Sijmons, R.H., Woods, D.G., *et al.* (1997). Germline mutations in the PTEN/MMAC1 gene in patients with Cowden disease. *Hum Mol Genet* 6, 1383-1387.

Noh, K.H., Kim, S.H., Kim, J.H., Song, K.H., Lee, Y.H., Kang, T.H., Han, H.D., Sood, A.K., Ng, J., Kim, K., *et al.* (2014). API5 confers tumoral immune escape through FGF2-dependent cell survival pathway. *Cancer Res* 74, 3556-3566.

Rahman, N., Seal, S., Thompson, D., Kelly, P., Renwick, A., Elliott, A., Reid, S., Spanova, K., Barfoot, R., Chagtai, T., *et al.* (2007). PALB2, which encodes a BRCA2-interacting protein, is a breast cancer susceptibility gene. *Nat Genet* 39, 165-167.

Ramdass, P., Rajihuzzaman, M., Veerasenan, S.D., Selvaduray, K.R., Nesaretnam, K., and Radhakrishnan, A.K. (2011). Tocotrienol-treated MCF-7 human breast cancer cells show down-regulation of API5 and up-regulation of MIG6 genes. *Cancer Genomics Proteomics* 8, 19-31.

- Ratajska, M., Antoszewska, E., Piskorz, A., Brozek, I., Borg, A., Kusmierk, H., Biernat, W., and Limon, J. (2012). Cancer predisposing BARD1 mutations in breast-ovarian cancer families. *Breast Cancer Res Treat* 131, 89-97.
- Reginato, M.J., Mills, K.R., Becker, E.B., Lynch, D.K., Bonni, A., Muthuswamy, S.K., and Brugge, J.S. (2005). Bim regulation of lumen formation in cultured mammary epithelial acini is targeted by oncogenes. *Mol Cell Biol* 25, 4591-4601.
- Reginato, M.J., and Muthuswamy, S.K. (2006). Illuminating the center: mechanisms regulating lumen formation and maintenance in mammary morphogenesis. *J Mammary Gland Biol Neoplasia* 11, 205-211.
- Renwick, A., Thompson, D., Seal, S., Kelly, P., Chagtai, T., Ahmed, M., North, B., Jayatilake, H., Barfoot, R., Spanova, K., *et al.* (2006). ATM mutations that cause ataxia-telangiectasia are breast cancer susceptibility alleles. *Nat Genet* 38, 873-875.
- Rhee, D.K., Park, S.H., and Jang, Y.K. (2008). Molecular signatures associated with transformation and progression to breast cancer in the isogenic MCF10 model. *Genomics* 92, 419-428.
- Rigou, P., Piddubnyak, V., Faye, A., Rain, J.C., Michel, L., Calvo, F., and Poyet, J.L. (2009). The antiapoptotic protein AAC-11 interacts with and regulates Acinus-mediated DNA fragmentation. *EMBO J* 28, 1576-1588.
- Santner, S.J., Dawson, P.J., Tait, L., Soule, H.D., Eliason, J., Mohamed, A.N., Wolman, S.R., Heppner, G.H., and Miller, F.R. (2001). Malignant MCF10CA1 cell lines derived from premalignant human breast epithelial MCF10AT cells. *Breast Cancer Res Treat* 65, 101-110.
- Sarrio, D., Rodriguez-Pinilla, S.M., Hardisson, D., Cano, A., Moreno-Bueno, G., and Palacios, J. (2008). Epithelial-mesenchymal transition in breast cancer relates to the basal-like phenotype. *Cancer Res* 68, 989-997.
- Sasaki, H., Moriyama, S., Yukiue, H., Kobayashi, Y., Nakashima, Y., Kaji, M., Fukai, I., Kiriya, M., Yamakawa, Y., and Fujii, Y. (2001). Expression of the antiapoptosis gene, AAC-11, as a prognosis marker in non-small cell lung cancer. *Lung Cancer* 34, 53-57.
- Seal, S., Thompson, D., Renwick, A., Elliott, A., Kelly, P., Barfoot, R., Chagtai, T., Jayatilake, H., Ahmed, M., Spanova, K., *et al.* (2006). Truncating mutations in the Fanconi anemia J gene BRIP1 are low-penetrance breast cancer susceptibility alleles. *Nat Genet* 38, 1239-1241.
- Song, K.H., Kim, S.H., Noh, K.H., Bae, H.C., Kim, J.H., Lee, H.J., Song, J., Kang, T.H., Kim, D.W., Oh, S.J., *et al.* (2014). Apoptosis Inhibitor 5 Increases Metastasis via Erk-mediated MMP expression. *BMB Rep.*

Swana, H.S., Grossman, D., Anthony, J.N., Weiss, R.M., and Altieri, D.C. (1999). Tumor content of the antiapoptosis molecule survivin and recurrence of bladder cancer. *N Engl J Med* 341, 452-453.

Tewari, M., Yu, M., Ross, B., Dean, C., Giordano, A., and Rubin, R. (1997). AAC-11, a novel cDNA that inhibits apoptosis after growth factor withdrawal. *Cancer Res* 57, 4063-4069.

Thompson, D., and Easton, D.F. (2002). Cancer Incidence in BRCA1 mutation carriers. *J Natl Cancer Inst* 94, 1358-1365.

Tinoco, G., Warsch, S., Gluck, S., Avancha, K., and Montero, A.J. (2013). Treating breast cancer in the 21st century: emerging biological therapies. *J Cancer* 4, 117-132.

Tomlinson, D.C., Baxter, E.W., Loadman, P.M., Hull, M.A., and Knowles, M.A. (2012). FGFR1-induced epithelial to mesenchymal transition through MAPK/PLCgamma/COX-2-mediated mechanisms. *PLoS One* 7, e38972.

Turnbull, C., and Rahman, N. (2008). Genetic predisposition to breast cancer: past, present, and future. *Annu Rev Genomics Hum Genet* 9, 321-345.

Van den Berghe, L., Laurell, H., Huez, I., Zanibellato, C., Prats, H., and Bugler, B. (2000). FIF [fibroblast growth factor-2 (FGF-2)-interacting-factor], a nuclear putatively antiapoptotic factor, interacts specifically with FGF-2. *Mol Endocrinol* 14, 1709-1724.

van Diest, P.J., and Baak, J.P. (1991). The morphometric prognostic index is the strongest prognosticator in premenopausal lymph node-negative and lymph node-positive breast cancer patients. *Hum Pathol* 22, 326-330.

Vidi, P.A., Bissell, M.J., and Lelievre, S.A. (2013). Three-dimensional culture of human breast epithelial cells: the how and the why. *Methods Mol Biol* 945, 193-219.

Wang, Z., Liu, H., Liu, B., Ma, W., Xue, X., Chen, J., and Zhou, Q. (2010). Gene expression levels of CSNK1A1 and AAC-11, but not NME1, in tumor tissues as prognostic factors in NSCLC patients. *Med Sci Monit* 16, CR357-364.

Welsh, P.L., and King, M.C. (2001). BRCA1 and BRCA2 and the genetics of breast and ovarian cancer. *Hum Mol Genet* 10, 705-713.

Wu, X., and Gallo, K.A. (2013). The 18-kDa translocator protein (TSPO) disrupts mammary epithelial morphogenesis and promotes breast cancer cell migration. *PLoS One* 8, e71258.

Wu, Y., and Zhou, B.P. (2008). New insights of epithelial-mesenchymal transition in cancer metastasis. *Acta Biochim Biophys Sin (Shanghai)* 40, 643-650.

Zhan, L., Xiang, B., and Muthuswamy, S.K. (2006). Controlled activation of ErbB1/ErbB2 heterodimers promote invasion of three-dimensional organized epithelia in an ErbB1-dependent manner: implications for progression of ErbB2-overexpressing tumors. *Cancer Res* 66, 5201-5208.

Zhang, Y., Yan, W., and Chen, X. (2011). Mutant p53 disrupts MCF-10A cell polarity in three-dimensional culture via epithelial-to-mesenchymal transitions. *J Biol Chem* 286, 16218-16228.

Zink, D., Fischer, A.H., and Nickerson, J.A. (2004). Nuclear structure in cancer cells. *Nat Rev Cancer* 4, 677-687.